Biomaterials Science

ROYAL SOCIETY OF CHEMISTRY

REVIEW

View Article Online
View Journal | View Issue

Cite this: *Biomater. Sci.*, 2022, **10**, 1647

Graphene quantum dot-porphyrin/phthalocyanine multifunctional hybrid systems: from interfacial dialogue to application

Sujata Sangam,[a,b] Simran Jindal, [a] Aakanksha Agarwal, [a] Basu Dev Banerjee,[c] Puja Prasad*[d] and Monalisa Mukherjee *[a,b]

Received 5th January 2022,
Accepted 23rd February 2022

DOI: 10.1039/d2bm00016d

rsc.li/biomaterials-science

Engineered well-ordered hybrid nanomaterials are symbolically at a pivotal point, just ahead of the long-anticipated transformation of the human race. Incorporating newer carbon nanomaterials like graphene quantum dots (GQDs) with tetrapyrrolic porphyrins (Pp) and phthalocyanines (Pc) is crucial for achieving exquisite molecular nanoarchitectures that are superior to their individual components. The outcomes of this, particularly in the case of graphene quantum dot-porphyrin/phthalocyanine (GQD-Pp/Pc) hybrids, remain comprehensively unexplored to date. Interestingly, GQD-Pp/Pc hybrids provide a modern strategy to regulate matter by utilising intramolecular and organisational properties to create well-defined nanocomposites *via* a synergistic enhancement effect. The high molar absorption coefficient and enhanced energy transfer, hole and electron transfer abilities capabilities allow Pp and Pc to exhibit a wide spectrum of photophysical and photochemical features. However, their low biostability, non-specific tumor-targeting properties, hydrophobicity, and low cellular internalisation efficiency limit their extensive biomedical utility. Conjugating Pp/Pc to nanocarriers such as GQDs improves their targeted delivery, immunological tolerance, and longevity. Due to the zero-order release kinetics of GQDs, they can assist in maintaining a steady rate of photosensitiser (PS) delivery at the desired site. To completely rationalise the functionalization of GQD-Pp/Pc species at interfaces, we investigate the current prominence and future potential of porphyrin-related graphene nanosystems, especially GQDs, for the development of various applications. This encouraging report demonstrates how GQD-Pp/Pc species can be used to examine new phenomena at the multidisciplinary level. Notably, a customised hybrid system optimises amendable and diverse functional properties, yielding a ray of hope in the fields of photodynamic therapy (PDT), photocatalysis, solar cells, sensing, and beyond *via* various photo-physicochemical approaches such as electron transfer, catalytic transformation, light-harvesting, and axial/peripheral ligation of adducts. Gratifyingly, the covalent and non-covalent coupling of functional molecular units at interfaces enable new properties to be generated in hybrid systems.

1 Introduction

The exploration and elucidation of structurally well-ordered nanocomposites by combining GQDs with optically active porphyrins (Pp)/phthalocyanines (Pc) affords new or enhanced functionalities aided by the synergistic conjugation of multicomponents, culminating in myriad applications at the forefront of rapidly expanding domains.[1–10] Substantial effort has been devoted to illuminating the innate properties of natural tetrapyrroles, *i.e.*, porphyrins (Pp), also called the "pigments of life", and their synthetic analogues, *i.e.*, phthalocyanines (Pc), depicting transformative milestones in biomimetic systems.[3,5,11–15] Due to their extensive delocalized π-electrons, Pp are vital molecules widely present in nature in the form of enzyme active sites and visible light absorption units, which offer a convenient opportunity to control matter at the nanoscale with impressive potential.[16,17] Pp and artificial Pc usually present surface and interface-related properties for various industrial and scientific applications.[11–13] However, the hydrophobic properties of Pp/Pc and their lack of biodistribution

[a]*Molecular Science and Engineering Laboratory, Amity Institute of Click Chemistry Research and Studies, Amity University Uttar Pradesh, Noida – 201313, India. E-mail: mmukherjee@amity.edu; Tel: +91(0)-120-4392194*
[b]*Amity Institute of Biotechnology, Amity University Uttar Pradesh, Noida – 201313, India*
[c]*Environmental Biochemistry & Molecular Biology Laboratory, Department of Biochemistry, University College of Medical Sciences & GTB Hospital, University of Delhi, Delhi 110095, India*
[d]*Department of Chemical Engineering, Indian Institute of Technology Delhi, Hauz Khas, New Delhi, 110016, India. E-mail: pujaprasadiisc@gmail.com*

due to their aggregation *via* the stacking of their planar molecules has shifted the focus of research to porphyrin–nanomaterial conjugated systems.[6,18]

Differentcarbon nanomaterials[19] elegantly integrated within the tetrapyrrole ligand are crucial for accomplishing various vital processes by constructing conjugates.[20–24] The analysis of new forms of carbon[25,26] has transmuted the horizon of nanostructures and opened new avenues for exploration.[10,27,28] In the graphene family, GQDs with a unique structure have become the focus owing to their huge potential in a variety of applications.[29–35] GQDs are zero-dimensional, sp^2-hybridized, fluorescent, semiconductor, carbon nanocrystals (typical size range of 3–30 nm), with the graphene lattices arranged in a honeycomb structure and joined *via* functional chemical groups on the edge/surface.[26,36–39] The interactions in GQDs-Pp/Pc[40] system provide new opportunities to achieve several synchronized adsorption conformations, with a change in substrate binding, electronic level alignment, charge-transfer,[29] axial/peripheral ligation (chemical), and magnetic features.[15,41,42] In the pursuit of new applications, the advantage of the systematically tuned functionalization of porphyrinic[43]-GQD complexes also offers customized and intricate supramolecular association[44,45] for the establishment of unique optical, geometrical, and electronic properties in biomimetic systems.[29] Therefore, Pp/Pc-based GQD nanohybrids, depending on the kinetics, environment, and other factors, show structure–function relationships. Nowadays, theoretical modeling, including principal component analysis (PCA), can rapidly reveal the distinctive signatures of the responses from nanohybrid systems and their components.[15,52] Unquestionably, the emergence of pragmatically designed, bio-inspired, semi-synthetic GQD-Pp/Pc derivatives will have a wide impact in the field of medical[53] treatment including drug development. Particularly, in PDT,[54] the optical properties and photosensitizer[55] can be enhanced to improve its efficacy with site-localized properties through curtailing the dose-limit side effects.[29,36,37,41,51,56] This will also avoid or abate chemical degradation in the physiological system.[57]

This review focuses on the challenges associated with GQDs and Pp/Pc[58] individually, providing insight into the development of GQD-Pp/Pc hybrid systems, which will exhibit advantages and unique features in many field, including energy (light-harvesting process),[59] catalysis, optical devices, sensors,[33] and therapeutics (Fig. 5).[13,60] The achievements in these domains have not yet been accessed comprehensively in a single study, particularly for GQD[37]-Pp/Pc system,[21] and thus we present examples and theoretical predictions. Gratifyingly, this outlook can inspire new paradigms and strategies in the application of GQD-Pp/Pc hybrids,[61] leading to their widespread advancement compared to their separate components. The impetus for the current work was based on the need for robust conjugation to achieve the synergistic enhancement of several features.[62–68]

Finally, we envisage the key issues to be overcome, future research directions, and perspectives to show a full picture of these hybrids, which will enable the scientific community to appreciate the versatile application and properties exhibited by GQD-Pp/Pc hybrid systems and further encourage work in this field to unveil the unexplored path.

1.1 Graphene quantum dots (GQDs)

Several nanoparticles have raised concerns about their difficult fabrication, unfavourable biodistribution, and limited ability to control the release of their payload. Furthermore, significant background noise and the lack of an amplification approach to boost the signal output of the target are important roadblocks in the advancement of nanoparticle imaging.[69] In contrast, the impressive progress achieved in graphene[70,71] chemistry has made GQDs the "golden targets" for future studies

Sujata Sangam

Sujata Sangam received her M. Sc. (Biotechnology) and M.Tech. (Environmental Engg. & Management) from SHUATS, Allahabad and IIT Kanpur, UP, respectively. Then, she joined Amity Institute of Biotechnology, Amity University (Noida), U.P., India, to pursue her Ph.D. She is currently involved with the Amity Institute of Click Chemistry Research and Studies (AICCRS). She is a recipient of the GATE and CSIR-UGC JRF Fellowship. Her current research interest focuses on the interfaces of molecular chemistry, nanotechnology, biotechnology, environmental engg. and studies based on biomimetic smart carbon-nanomaterials, hydrogels, nanocomposites and their biomedical applications.

Simran Jindal

Simran Jindal is currently pursuing her M.Sc. in Molecular Chemistry from the Amity Institute of Click Chemistry Research and Studies, Amity University (Noida), U.P., India, after receiving her undergraduate degree from Delhi University, India. Her research interests include green chemistry, nanocomposites, and their relevance in biological application.

due to their cutting-edge properties.[72–79] GQDs have the fascinating characteristics of both two-dimensional (2D) graphene and the exceptional physicochemical properties of QDs, namely, quantum confinement effect, non-zero bandgap, and edge effects.[34,80–83] Graphene-based quantum dots (GQDs) have been comprehensively explored due to their desirable attributes such as facile, eco-friendly synthesis, low cost, non-toxicity, good biocompatibility,[36,84,85] high stability, controllable chemical functionality, water dispersibility, surface grafting, stable photoluminescence,[73] robust chemical inertness,[26] excellent electrical, and optical properties, abundant functional groups (*e.g.*, hydroxyl, amino, and carboxyl), electron mobility, and huge surface area, endowing them immense potential applications in the optical,[86] energy,[87] electronic, and biomedical fields.[88,89–96]

Owing to their quantum confinement and special edge effects, GQDs show distinct fluorescent properties and physical and chemical properties.[32,33,97–100] The size of their π-conjugated regions and their surface/edge structures regulate their optical properties, while maintaining their anisotropic nature, *i.e.*, lateral dimensions greater than their height.[26,101] Interestingly, GQDs are superior to get engineered at bio-interfaces. Besides being dimensionally wise compatible with the redox active sites within tunneling distance of cofactors, they considerably decrease the oxygen adsorption and the electron transfer barrier,[23] providing enhanced electron transfer, electronic conduction abilities, and electrocatalytic activity for the redox reaction (ORR) due to the increased contribution of electro-catalytically active edge sites.[15,36,102,103] Some of these properties have spurred a wide range of potential applications[104] of GQDs in photodetectors, fluorescent agents,[73,91] solar cells, bioimaging,[91] sensors,[105] batteries, light-emitting diodes (LEDs), electro-/photo-catalysis, drug delivery,[106] *etc*.[36,37,77,78,86,107–111]

Not geometrically, but functionally, GQD can be compared with graphene oxide (GO), whose surfaces/edges are usually decorated with carbonyl, hydroxyl, carboxyl, and/or epoxide groups.[24,27,43,112–115] With these functional groups, GQDs display amphiphilicity, wherein their core is hydrophobic, while their periphery tends to be hydrophilic, resulting in excellent interfacial activity for dispersing agents or producing Pickering emulsions.[116–118] Usually, graphene-based oxides are toxic and poorly fluorescent, and thus GQDs can be used to solve these problems due to their excellent physicochemical properties.[119]

1.2 Porphyrin/phthalocyanine

Porphyrins, together with the artificial phthalocyanines, have numerous scientific and technological applications,[120,121] which often involve surface/interface-related features because of their size, complexity, remarkable stability, specific ligand functionality, and planar structures of their parent macrocycles.[3,11,12,15,21] The planar arrangement of Pp and Pc is beneficial for adsorption *via* substantial van der Waals interactions, given that it brings other atoms into adjacent proximity to the substrate.[15] Pp has distinctive photophysical properties and is extremely stable, with a sharp Soret band and enormous extinction coefficient, together with another characteristic absorption (550 to 700 nm) extending from the ultraviolet (UV) to near-infrared (NIR) region[122,123] (Fig. 1a). These attributes make porphyrins valuable for the creation of functional nanostructures with donor–acceptor assembly for photo-

Aakanksha Agarwal

Aakanksha Agarwal received her Master's Degree from the State University of Uttarakhand, India. Currently, she is pursuing her PhD in Molecular Sciences and Engineering from the Amity Institute of Click Chemistry Research and Studies (AICCRS), Amity University, Noida, India. Her current research focuses on the synthesis and characterization of polymer nanocomposites, carbon-based nanomaterials and recent advances towards the sustainable production of biomass, lipids, proteins and bioactive components from microalgae using heterogeneous nanomaterials.

Basu Dev Banerjee

Professor Banerjee is an eminent Indian toxicologist and is ranked among the top 2% of global scientists from India, as stated by a Stanford University study (Updated science-wide author databases, Plos Biology, 2020). Dr B. D. Banerjee is currently working as a Professor of Biochemistry at the Department of Biochemistry, University College of Medical Sciences, since November 2000. He is actively involved in the areas of biochemistry, toxicology/toxicogenomics, immunotoxicology, environmental health and biology. Specifically, he has developed expertise in one of the thrust areas of 'xenobiotic-induced immunomodulation and neurotoxicity' during his career and contributed immensely to this subject in the last 38 years. His research concentrates on the identification of xenobiotic exposure/environmental stressors in microwave-induced genotoxicity and neurotoxicity in rat models as well.

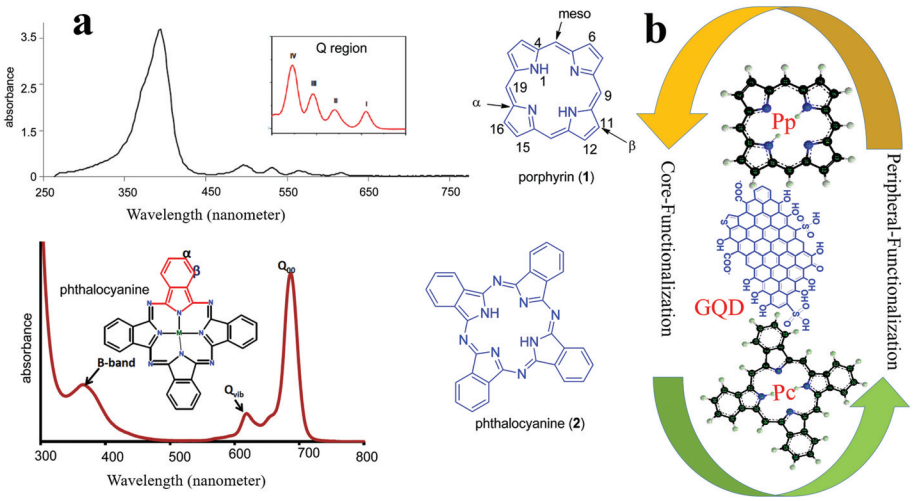

Fig. 1 (a) Porphyrin (Pp) and phthalocyanine (Pc).[11] © Copyright, Advances in Natural Sciences: Nanoscience and Nanotechnology 2014. (b) Core and peripheral functionalization of macrocycles (Pp/Pc) with GQDs.

catalysis, PDT, solar energy conversion, and molecular electronics.[124]

Primordial bioinspired molecules, *i.e.*, porphyrinic macrocyclic tetrapyrrolic arrangements joined by methine units, remain ubiquitous and invaluable in nature, acting as good photosensitizers.[15] Phthalocyanines consist of four isoindole units linked by nitrogen atoms, similar to the structure of porphyrin, but different due to the presence of nitrogen in place of carbon in the methylene linker.[2,14,15] Subsequently, the absorption spectrum of Pp and Pc differs in the near-infrared region. Pp and Pc porphyrinoids[13,60] with graphene-based carbon nanomaterials are prominent in the scientific frontier.[125,126] Pp and its synthetic analogs, Pc,[127,128] are thermo-chemically stable compounds with rich redox chemistry, which can be simply tailored by careful selection of the metal atom in the macrocyclic cavity and/or by placing appropriate substituents at the peripheral and/or axial positions of the macrocycle[10,21,71,124,129–131] (Fig. 1b). The nitrogen atoms in the interior form an anionic center in the central pocket, which are ideally positioned to coordinate unsaturated units for charge transfer and ligation of adducts, with reversible changes in their electronic configuration, for example, oxidation or spin states.[15] In surface science, Pp with robust functionalities exhibit suitable reactivity, electronic, and magnetic properties.[10] The properties of Pp can be governed by (i) the insertion of a carbene into the metal–nitrogen bond of a met-

Puja Prasad

Puja Prasad obtained her BSc and MSc from Calcutta University and IISc Bangalore, respectively. She received her Ph. D. in 2014 from IISc Bangalore under the supervision of Prof. Akhil R. Chakravarty, where she worked on the design and synthesis of metal-based anticancer agents. She then joined the group of Prof. Patrick J. Sinko, Rutgers University, USA, for her postdoctoral research from 2014 to 2015. Currently, she is working as a CSIR-Senior Research Associate in the Department of Chemical Engineering, IIT Delhi, India. Her research interests include the development of nano-bio conjugated systems and metal-based complexes for combatting antimicrobial resistance.

Monalisa Mukherjee

Prof. Monalisa Mukherjee completed her Bachelor's and Master's Degrees from the University of North Bengal, India. She received her Ph.D. from CBME, IIT Delhi, in 2006. Presently, she is serving as the Director of the Amity Institute of Click Chemistry Research and Studies (AICCRS) & Professor at the Amity Institute of Biotechnology, Noida, India. She is also a recipient of the UK-India Distinguished Visiting Scientist Award. She was admitted as a fellow of the Royal Society of Chemistry (FRSC), London, UK, in 2021. During the past 5 years, Dr Mukherjee has made exemplary contributions to the field of materials science. Her research is not only reinforced by her translational and potential work but also her remarkable publications and patents.

alloporphyrin (MP), (ii) substitution at the *meso*- and α/β (peripheral)-positions, central transition metal ions, and metal ion axial ligands, and (iii) insertion of a carbene in a free-base ring to form an *N*,*N*′vinyl-bridged porphyrin[16,27] (Fig. 1b). These efforts culminated in seminal explorations of porphyrins to improve their use in energy, PDT, biomimetic catalysis, photocatalysis, electrocatalysis, sensing, semiconductor, sensor, electrophotography, supramolecular chemistry, and biomedical[55,132] applications[8,10,15,46,55,71,133–138,139–143] (Fig. 5). The presence and type of central metal ion with axial ligands, the peripheral decoration, and the ring microenvironment all influence the optical, catalytic, electrochemical, and photochemical properties of porphyrins.[144] For both PDT and solar cell applications, it is essential that electron promotion to the lowest excited state be achieved by the absorption of red light.[6,145] In the case of energy, chirality is also interesting because of the chiral-induced spin selectivity (CISS) effect.[146]

1.3 Why porphine-based GQD nanocomposites?

Notably, pure GQD suffers from problems related to poor conductivity, difficult assembly into films, low quantum yield (ϕ), *etc*.[29,104,147] Given that quick electron–hole recombination turns electronic energy into thermal energy, the photoluminescence (PL) quantum yield of GQDs is often reduced. Alternatively, the functionalization of GQDs can minimise their vibrational relaxation and increase their PL, ϕ.[148] GQD composites also enhance the efficiency of the device.[2,36,74] Porphine, sometimes known as porphin, is the simplest of the tetrapyrroles, which is made up of four pyrrole-like rings connected by four methine groups to form a bigger macrocycle ring.[149] Although Pp-based derivatives are unquestionably the most suitable ligands for biological applications,[3,43,143,150] they have a number of disadvantages such as insolubility in water, skin photosensitivity, dark toxicity, reduced depth of tumor necrosis, excruciating pain during photo-irradiation, and multistep synthesis for some photosensitizer formulations.[5,8,151,136] The most promising application of porphyrinic compounds is PDT due to their low cytotoxicity and efficient generation of ROS.[3,137,138] Besides, Pp/Pc are also well-known for their photocatalytic properties because of their homogeneous nature in solution, but they suffer from problems related to poor recovery and reusability, *etc*.[71,152–154] These problems can be easily circumvented by constructing a hybrid system of GQDs-Pp/Pc *via* interface engineering, overcoming the inherent problems associated with porphyrinic compounds and enhancing the efficacy of GQDs for various applications.[131,155–158,193]

The functionalization of GQDs is an efficient strategy to enhance the basic properties of nanocomposites, resulting in several additional optico-physicochemical properties for wider applications.[1,42,43,85,103,159,160] Currently, porphyrins are applied in optics and medicine, such as nonlinear absorbers or PDT, which increasingly require the use of far-red absorbing dyes.[136,161] Accordingly the porphyrin framework can be modified to achieve this, including conjugation of the porphyrin π-system, which results in a bathochromic shift in the absorption spectrum.[27,161,162] Thus, the conjugated porphyrin framework has extensive applications. If the inherent properties of porphyrin macrocycles, that is, metal centres capable of axial ligation of adducts, are preserved upon coupling with graphene, further options for the functionalization of graphene-based nanostructures, namely, GQDs, emerge.[15,163] These nanostructures are crucial in various prosthetic groups, carrying out vital functions for bioenergetic pathways.[164] The favorable findings have been attributed to the ability to conjugate graphene nanomaterials with Pp/Pc to overcome the barriers to both pharmacologic and molecular mechanisms.[22,51,107,109] These hybrids also mediate intricate catalytic conversions and the transport or storage of respiratory gases. Furthermore, they exhibit strong optical[91,165] absorption in the red/near-infrared (NIR) region of the solar spectrum, resulting in near-perfect light-harvesting units,[67] which are ideal components for PDT[166] and photoelectronic devices.[38,136]

Consequently, GQD-Pp/Pc hybrid-based materials as functional molecular units are usually applied in homogeneous systems. The heterogeneity of these moieties in crystalline frameworks with long-range-ordered structures will help facilitate their recyclability, and more importantly, understand their structure–property relationships.[15,123,167–171]

2 Construction of GQD-porphyrin/phthalocyanine hybrid systems

Recently, porphyrins stemmed from investigations as components of functional nanomaterial assemblies, highlighting the structural-functional correlation of a nanocrystal, wherein the interparticle spacing and orientation of building blocks can provide new function.[24,43,68,172,173]

Given that the interaction of the extended π-electron network of porphyrins with graphene results in interesting optoelectronic properties, the covalent and non-covalent chemistry of porphyrins with graphene-based nanomaterials has been widely investigated.[27,64,110,112,163] However, there are major obstacles in obtaining nanocrystals with structural-compositional complexity,[174] which require conserving the desired monodispersed property, without hampering accessibility to the innate properties of the Pp/Pc building blocks for their use. The covalent functionalization of porphyrin-nanotube conjugates can be accomplished through linkages such as carboxylic acid-induced esterification, Suzuki coupling, azide–alkyne Huisgen cycloaddition (1,3-dipolar cycloaddition), and diazonium chemistry on a pre-functionalized nanotube surface.[46,53,144] This implies that Pp/Pc can be conjugated to GQDs *via* covalent bonds using common organic reactions such as amide coupling, click chemistry, and Michael addition reactions (Fig. 2a and b).

Additionally, iridium- or palladium-catalyzed direct C–H functionalization of Pp is emerging as an efficient way to introduce various functional groups in porphyrins. Furthermore, the copper-mediated Huisgen cycloaddition reaction has become a common approach to incorporate porphyrin units

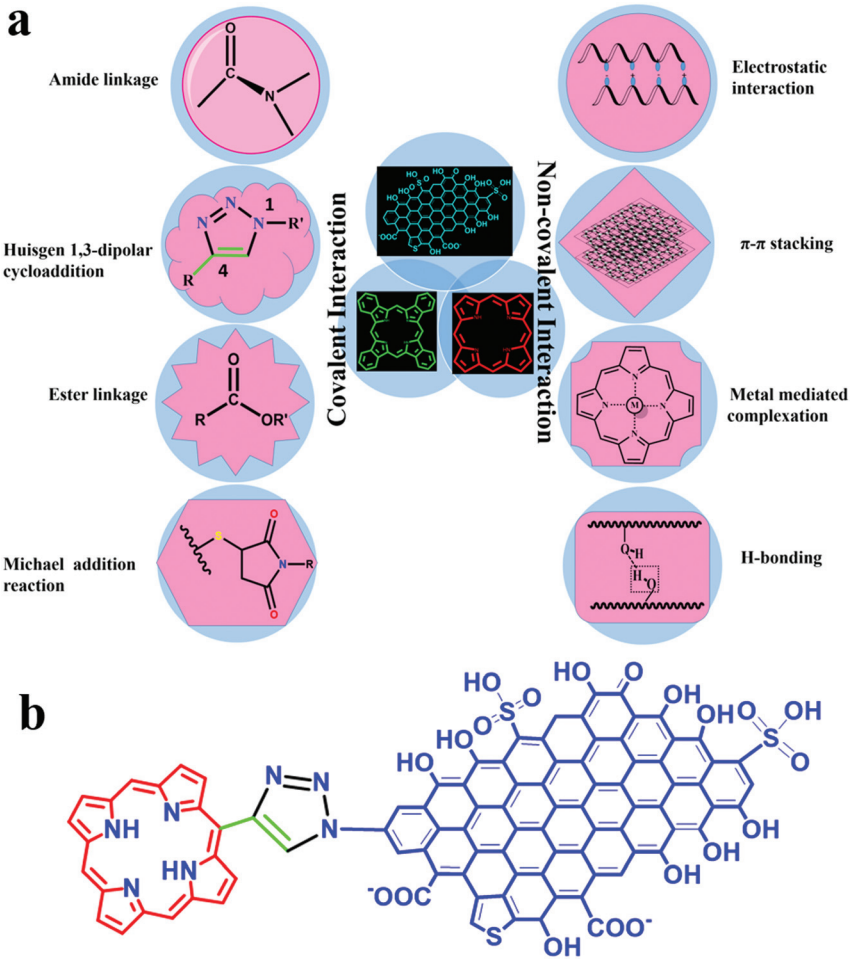

Fig. 2 (a) Types of interactions between the tetrapyrrole ring and GQDs. (b) Click reaction of a macrocycle with GQDs.

into functional graphene sheets. Now, these techniques, together with the traditional porphyrin synthesis, can help to construct a wide range of highly elaborate and complex Pp architectures. Based on their photophysical and electrochemical properties, GQDs and tetrapyrrole rings have been considered for active research, especially to understand the electron transfer and energy transfer processes in photosynthesis. The Cu(I)-catalyzed azide–alkyne cycloaddition (CuAAC) reaction may significantly simplify the preparative paths to Pp/Pc molecules, although the assembly of covalently conjugated Pp/Pc[58] usually requires complex synthetic procedures. Click chemistry[175] is a powerful tool to access Pp architectures. Furthermore, the mechanism of the photoinduced electron transfer may be investigated using a diverse range of Pp-GQD conjugates. Click chemistry can be used to functionalize GQDs with diverse organic compounds, allowing the creation of a high molecular weight material in a single step (Fig. 2b).

The functional groups on the peripheries of Pp are important in the combination mode of Pp/Pc and GQDs. Multifunctional nanometer-scale architectures for optical/optoelectronic applications and catalysis have been explored, which combine the properties of the solution-dispersible form of graphene (graphene oxide) and porphyrins.[56,176,177] The achieved photophysical properties reveal a remarkable optical limiting effect, *i.e.*, high transmittance of low-intensity light and attenuation of intense optical beams.[53,110,178,179] Due to the limited potency and various side effects associated with most non-porphyrinoid PS, the application of tetrapyrrole in PS is highly necessary. Covalent interaction provides thermodynamic stability to the structure. However, bond formation disturbs the electronic configuration of the material.[43,68,115,163] In the covalent approach, GQDs are first activated to obtain the required functional groups such as –COOH or $–NH_2$ on the surface of GQDs, and then reacted with Pp/Pc to obtain a stable bond (Scheme 1a). Alternatively, carboxylic acid-functionalized metallophthalocyanine (MPc) can be activated and conjugated to amine-functionalized GQDs to form an amide linkage.[180] In their pioneering work, Wang *et al.* studied the chemical functionalization of carbon-nanotubes (CNTs) and graphene for real-world applications.[21]

In the covalent approach, the π-delocalized linkage in graphene/CNTs is perturbed, resulting in the formation of defects, diminishing their stability and conductivity, and improving their solubility and optoelectronic applications.

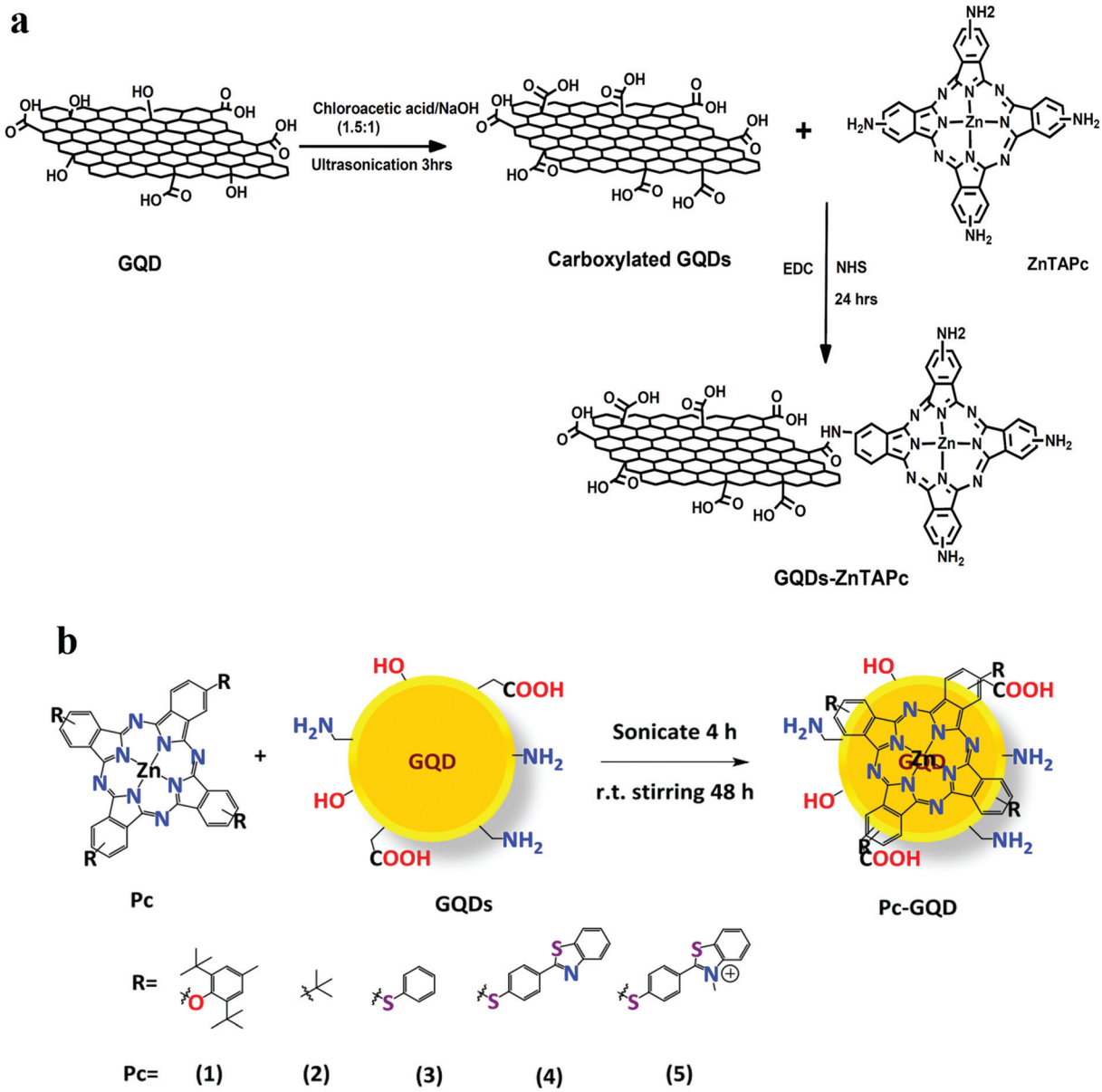

Scheme 1 (a) Covalent linkage of GQDs and ZnTAPc *via* amide coupling.[180] (b) Schematic diagram depicting π–π stacking between Pc and GQDs.[302] (c) Non-covalent interactions of GQDs and ZnTCPPc/ZnTmPyPc *via* π–π stacking and ionic interaction.[180] © Copyright 2016 and 2019, Elsevier.

Additionally, the functionalization of graphene moieties *via* free radical addition promotes the opening of the bandgap and tweaks the solubility of graphene.[21] On the contrary, non-covalent functionalization of CNTs with porphyrins results in the introduction of various Pp/Pc without disturbing the aromatic character and electronic configuration of the graphene framework[170,182] (Scheme 1b and c). Menilli *et al.* discovered that cationic porphyrins are more easily internalised than their non-cationic counterparts and their positively charged structures allow non-covalent bonding with both GQDs and GO at physiological pH. The absorbance of porphyrins was typically red-shifted when they were titrated with GO using spectrophotometric and spectrofluorometric methods, and the original fluorescence was quenched. The incredible features of GQD-Pp/Pc are based on biomimetic organization principles *via* non-covalent interactions such as metal-mediated complexation, hydrogen bonding, electrostatic interaction, π–π stacking, and van der Waals. These non-covalent interactions can govern the stability and geometry of nanohybrids, and also significant in controlling their structure and electron transfer properties[24,43,44,123,143,183] (Fig. 2 and Scheme 1b, c) However, these nanohybrids have stability issues given that they suffer from weak interactions between the GQDs and porphyrin units, often leading to the loss of their porphyrin units.

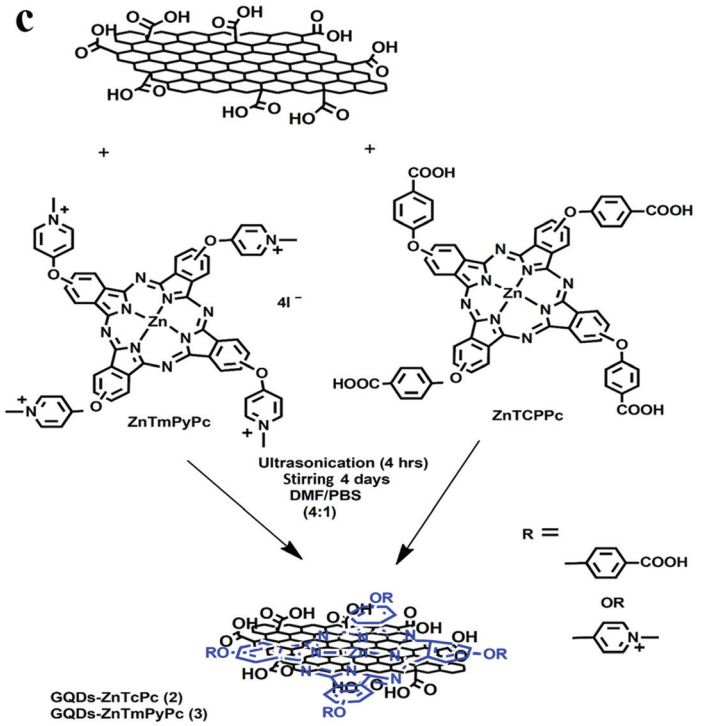

Scheme 1 *(Contd).*

According to Pallikkara *et al.*, covalent functionalization is a difficult and low-yielding technique, whereas non-covalent functionalization is simple and versatile.[184]

He *et al.* investigated the controlled modification of surface-anchored nanographene and graphene nanoribbons *via* decoration with porphine, which is anticipated to play a significant role in diverse fields.[163,185] The size of a nanoparticle is perhaps its most basic attribute, besides its components.[186] The size of these hybrid GQDs is comparable with that of biomolecules, thereby providing an ideal platform to study biomolecules such as proteins, cells, and viruses.[24,187,188]

2.1 Methods to construct GQD-Pp/Pc hybrid systems

The methods for the synthesis of GQDs can currently be divided into the top-down and bottom-up approaches. To produce nano-quantum dots, bulk carbon materials such as graphene and carbon black are typically cracked *via* chemical/electrochemical exfoliation, hydrothermal/solvothermal treatment, and microwave/ultrasonic treatment in the top-down synthesis method, whereas in the bottom-up synthetic approaches, chemical reactions such as step-by-step organic synthesis are used to convert organic small molecules (such as citric acid (CA), fullerenes, and polycyclic aromatic hydrocarbons) or organic precursors into high-quality quantum dots.[85] One approach to build functional multi-component systems involves the lateral anchoring of organic heteromolecules to graphene.[163,189,190] This process enables the combination of graphene nanostructures with porphyrin to create hybrid systems with desirable and tunable functionalities at their interfaces.[15,27,43,163,191] In the study by Magaela *et al.*, propanoic acid was heated to 120 °C and refluxed with 2-(4-morpholinyl) benzaldehyde in the presence of 4-(4-morpholinyl) benzaldehyde. The mixture was then added to pyrrole and refluxed, and cooled to precipitate the porphyrin, giving a yield of 78%[192] (Scheme 2a). Santos *et al.* employed two distinct synthetic approaches to covalently functionalize GQDs with aminoporphyrin **1**. Using the thionyl chloride ($SOCl_2$) and 1-ethyl-3-(3′-dimethylaminopropyl) carbodiimide (EDAC) coupling methods, GQDs were coupled with an aminoporphyrin *via* an amide linkage. The carboxylic groups at the edges of the GQDs were transformed into acid chlorides using $SOCl_2$ before being coupled with porphyrin **1** to create the necessary amide group *via* A. The GQDs were first treated with chloroacetic acid to provide extra carboxylic functions, followed by conjugation with porphyrin **1**, utilising EDAC as the carboxyl activating agent *via* B. The EDAC process (*via* B, 63%) gave a greater reaction yield than the $SOCl_2$ procedure (*via* A, 43% yield). However, the $SOCl_2$ technique resulted in a better porphyrin loading based on structural characterization (Fourier transform infrared and X-ray photoelectron spectroscopy)[18] (Scheme 2b).

2.2 Characterization of GQD-based porphyrin hybrid systems

Pp/Pc, GQDs, and their hybrids present multiple options to govern their optical, electronic, and magnetic properties *via* easy and well-established synthetic methods.[39] UV/Vis spectroscopy, electrospray ionization (ESI) and MALTI-TOF mass

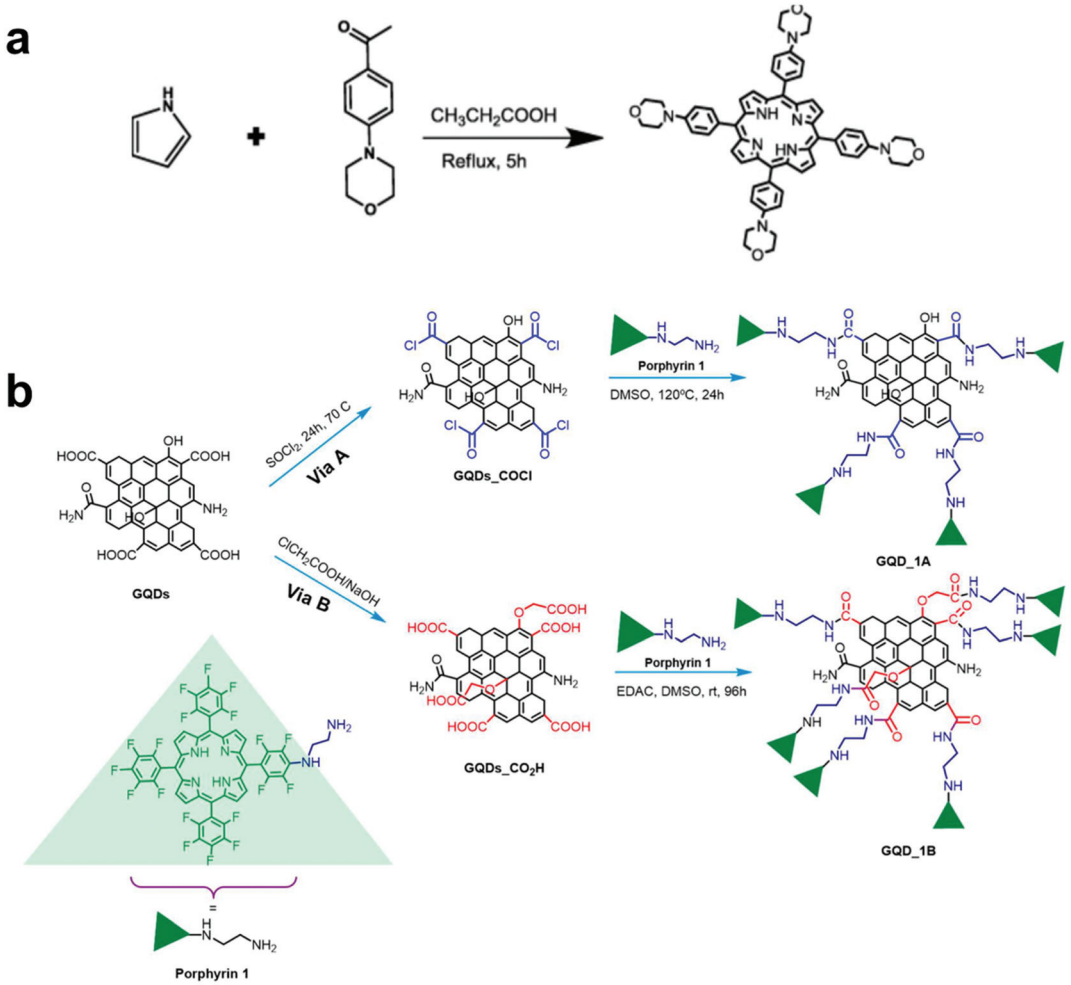

Scheme 2 (a) Synthetic pathway of porphyrin complex **1**.[192] Copyright 2015, Wiley-V.V. (b) Illustration of the two synthetic routes (*via* A and B) investigated for the preparation of two different types of GQD hybrids, namely GQD-1A and GQD-1B.[18] Copyright 2021, ACS.[18]

spectrometry, Raman spectroscopy, elemental analysis, Fourier-transform infrared spectroscopy (FT-IR), ^{1}H NMR spectroscopy, transmission electron spectroscopy (TEM), and dynamic light scattering (DLS) are used to characterize GQD-Pp/Pc nanohybrid systems.[119] DLS equipment can measure the size and size distribution of nanoporphyrin (NPs).[194] Transmission electron microscopy (TEM) and atomic force microscopy (AFM) were used to analyze the surface morphologies, lateral dimensions, and height distribution of a GQD-Pp/Pc hybrid system.[194] The functional groups or conjugation in porphyrins can be characterized *via* FTIR spectroscopy. The photophysical methods include UV-visible spectroscopy, fluorescence emission spectroscopy, and time-correlated single photon counting (TCSPC). Furthermore, the electron transfer dynamics can be obtained from TCSPC.[184] The zeta potential measures the charges in GQDs and GQD-Pp/Pc hybrid systems and helps to confirm the conjugation between GQDs and Pp/Pc. X-ray diffraction (XRD) is used to measure the disorder and defects in hybrid systems. X-ray photoelectron spectroscopy (XPS) is used to investigate the chemical composition of hybrid systems. Fluorescence spectrometry can be used to measure fluorescence signals and the absorbance of NPs.[194] Nene *et al.* reported that GQDs are monodispersed in their pristine form and tend to cluster when conjugated to Pc (TEM images). The average size for the non-conjugated GQDs determined from TEM imaging was ~9 nm, which increased upon conjugation to about ~19 nm for the GQD-Pc hybrid. The increase in size could be due to aggregation.[181] GQDs display diagnostic Raman bands namely, G and D bands, arising from the E_{2g} tangential vibrational mode of the sp^2-bonded carbons and disordered A_{1g} breathing vibrational mode of the aromatic sp^2 carbon rings, respectively. A shift in the G and D bands is generally considered a good factor for the characterization of the mode of binding of Pp/Pc with GQDs. There is minimal or no shift in the G and D band in the case of non-covalent bonding through π–π stacking of Pp/Pc and GQDs, whereas there is a large shift in the case of a covalently bound hybrid system.[41,131,195]

Recently, Menilli *et al.* reported that the inner filter effect (IFE) of Pp on GQDs produces significant fluorescence quench-

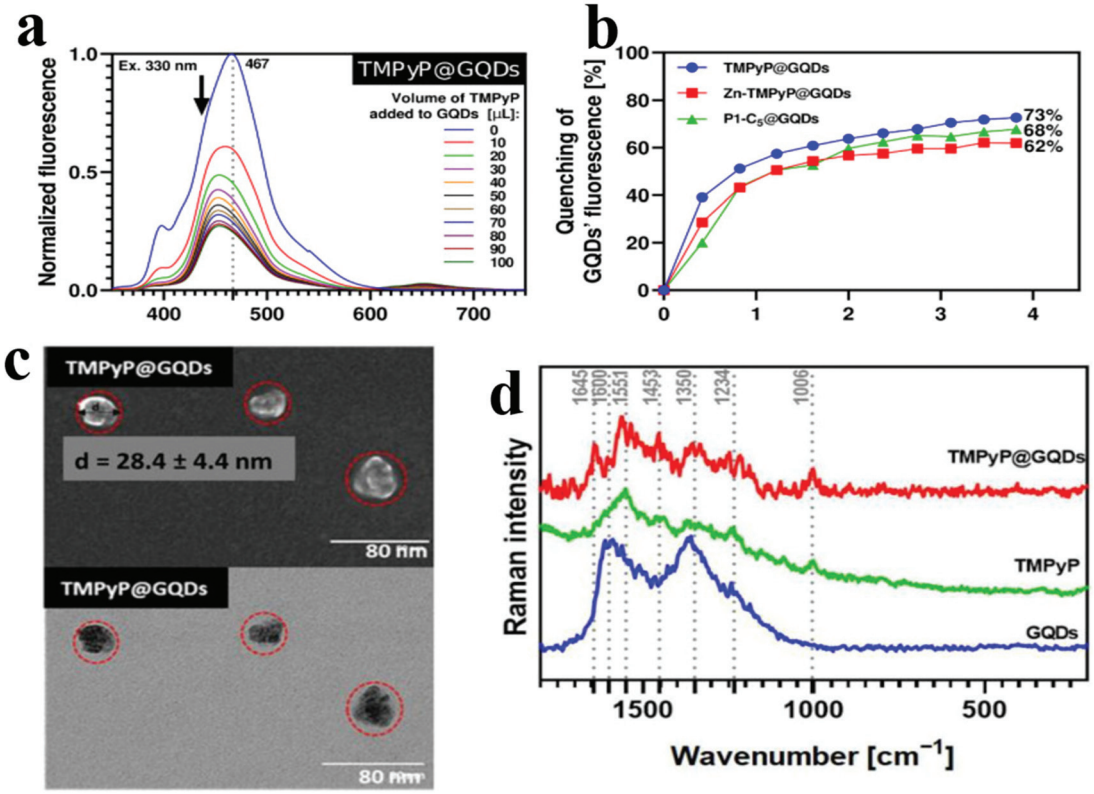

Fig. 3 Normalized fluorescence spectra of TMPyP@GQDs in aqueous solution at 330 nm with 10 min intervals. The spectra were produced by adding the porphyrin solution (42 M) to a 0.1 μg mL^{-1} GQD solution. (b) Porphyrins quench the GQD fluorescence (λ_{exc} = 330 nm). Under a 366 nm lamp, GQDs lose their fluorescence. (c) STEM images of TMPyP@GQDs. The red dotted lines represent the microscopically detected TMPyP@GQDs hybrid. (d) Raman spectra of free GQDs (blue), TMPyP (green), and TMPyP@GQDs (red line).[119] Copyright 2021, MDPI.

ing in GQDs upon conjugation because the Pp absorption bands are close to the emission bands of GQDs at the given excitation wavelength (Fig. 3a and b). The conjugation of GQDs with Pp increased the particle average size slightly (28.5 ± 4.4 nm) in the TMPyP@GQD hybrid (Fig. 3c). The Raman spectrum of the TMPyP@GQD hybrid exhibited features of both GQDs and 5,10,15,20-tetramethyl(4-pyridyl)porphyrin (TMPyP) (Fig. 3d). These findings imply non-covalent interactions between the TMPyP molecules and GQDs. All three hybrids provided Raman results that could be similarly interpreted.[119] According to Managa *et al.*, DLS data demonstrated that GQD nanoconjugates are larger than GQDs alone, indicating the creation of supramolecular assemblies of GQDs and porphyrins.[196]

3 Effect on photophysical properties due to GQD-Pp/Pc hybrid nanocomposites

Broad knowledge on the complex multicomponent architectures of GQD-Pp/Pc hybrids remains unclear in terms of photophysical behavior including electron transfer dynamics.[5,130,142,167,168,197] Porphyrins can easily govern their conformation to comply with their local environment *via* reorientations of their axial/peripheral ligands and macrocycle deformations, which are usually induced by molecule–substrate interactions.[163,169,198] The center-oxidized configurations of GQDs cause a larger perturbation in their conjugated π-system, reducing their band gap, and causing a redshift in their absorption spectrum. For some center-oxidized configurations, the addition of solvent causes red shifts in their absorption spectrum and increased intensities. In the absorption spectrum of edge-oxidized configurations, only red-shifts occur. The placement of the hydroxyl group in the basal plane of GQDs accelerates non-radiative decay, whereas that at the edges suppresses non-radiative decay. The current observation sheds light on the relationship between the surface chemistry and photoluminescence efficacy of GQDs.[148] Depending on the modes of interaction and bonding, two types of bonding interactions, *i.e.*, covalent and non-covalent, arise in GQD/Pp composites, especially in their absorption and fluorescence spectrum studies.[27,52,71,82,131,133,142,199–202] For instance, Xue *et al.* chosen three porphyrins with different functionalities to understand the interaction and bonding modes between GQDs and Pp.[1] Consequently, the red-shift in the Soret band and the new broad Q-band suggest that the edge and the surface of

GQDs play an important role in the π–π interaction of Pp and GQDs. The fluorescence of GQDs is quenched by Pp, and simultaneously the emission properties of Pp are efficiently enhanced due to Förster resonance energy transfer (FRET) or non-radiative dipole–dipole coupling.[124] Similar findings were reported by Achadu *et al.*, where GQDs were bound to ZnPc covalently (amide coupling) or non-covalently (π–π or electrostatic) to check their fluorescence behavior.[203] The FRET efficiency is dominant for covalent bonding compared to non-covalent conjugates given that the former mode of bonding results in closer proximity or stronger bonding between two molecules.[180] Thus, these synergistic properties of GQD and porphyrins/Pcs provide insight into their host–guest molecular assembly and have application in various fields.[37,204] The potential applications of GQD-porphyrin/Pc hybrid systems in PDT and photocatalysis depend on the high quantum yield (ϕ) of $^1O_2$.[66,205–207] For this, the effective transfer of energy from the T_1 state of these systems to the S_0 state of molecular oxygen is important for efficiently generating $^1O_2$. The updated Jablonski figure (Fig. 4) shows the main photochemical reactions prevailing in PDT. Photosensitizers can be excited from the ground state (S_0) to the excited singlet state (S_1) by an appropriate wavelength of light.[207] Among the three factors in PDT (photosensitizer, light, and oxygen molecules), the photosensitizer is the most important, given that it has a direct impact on the PDT efficiency. Intersystem crossover can either relax the excited photosensitizer back to the S_0 state with fluorescence photon emission or change it to an excited triplet state (T_1). A phosphorescent photon can relax the energy of a photosensitizer in the T_1 state or transfer it to ambient molecules *via* photochemical reactions of type I and II. By interacting with water or oxygen molecules, hydroxyl radicals ($OH^{\bullet}$) or superoxide anions ($^{\bullet}O_2^-$) are produced. Notably, type-I PDT can occur in hypoxic conditions, particularly in deep-seated tumor microenvironments. The toxic singlet oxygen ($^1O_2$) is formed when well-oxygenated photosensitizers in the T_1 state participate in an energy-transfer process with localised $^3O_2$. The PDT process is considered to be dominated by the type II path. However, high photosensitizer concentrations and hypoxia can favour the type I PDT pathway. Due to its non-invasiveness and spatiotemporal control, PDT is a promising anticancer approach[151] (Fig. 4).

Pallikkara *et al.* revealed that in GQD/Pp system, the HOMO and LUMO levels of Pp are above the energy levels of GQDs. Hence in the hybrid system, GQDs act as electron acceptors, whereas Pp as electron donors.[184] Notably, the mode of conjugation of porphyrin or phthalocyanine plays a vital role in the generation of quantum yield.[148,208] Nyokong *et al.* reported a detailed study on the type of linkage efficiency between covalent bonding and non-covalent bonding to GQDs.[209,210] This was demonstrated by designing a nano-construct of GQD/Pc supports in a photoactive membrane, where Pc is conjugated to GQD *via* covalent bonding ((c)Pc-GQD) and π–π stacking ((π)Pc-GQD). The results showed that the triplet quantum yield (ϕ_T) for (π)Pc-GQD is higher than that for (c)Pc-GQD due to the intramolecular rotational flexibility of Pc in the covalent conjugate. However, despite the higher ϕ_T of (π)Pc-GQD compared to (c)Pc-GQD, its singlet oxygen quantum yield (ϕ_Δ) is lower due to the screening effect caused by the GQDs, which prevents the interaction of the excited triplet state of conjugates with the ground state of molecular oxygen.[209] Thus, covalent linkage to GQDs is beneficial and may even be the most profitable way to use conjugates in PDT or photocatalysis.

4 Applications of GQD-Pp/Pc conjugates

Pp/Pc-based GQD nanohybrids can be implemented in a myriad of applications based on photosensitizers (PSs) for PDT,[46,47] photocatalysis, electrocatalysis, and sensing[48,49] due to the biomimetic photophysical, electrochemical,[50] and bioactive characteristics of Pp with improved efficacy[2,51] (Fig. 5).

4.1 Sensing

GQDs as sensors have been used for the quantitation of biomolecules, metal ions, and organic molecules but usually lack greater selectivity and sensitivity than other reported probes, mainly due to their low affinity and low quenching efficiency because of their poor induction by the analyte of interest.[1,10,211] In contrast, based on specific molecular recognition, GQD-Pp[2] nanocomposites with surface modification display enhanced selectivity in imaging, anticounterfeiting,

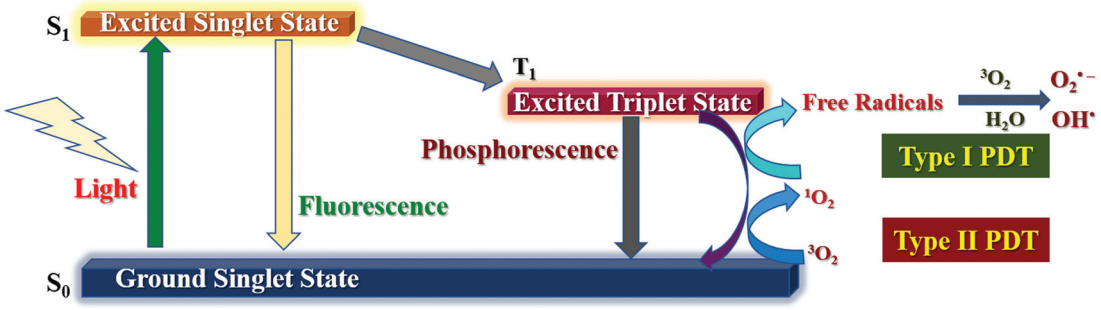

Fig. 4 Updated Jablonski diagram depicting reactive oxygen radical formation in type I and type II PDT.[151]

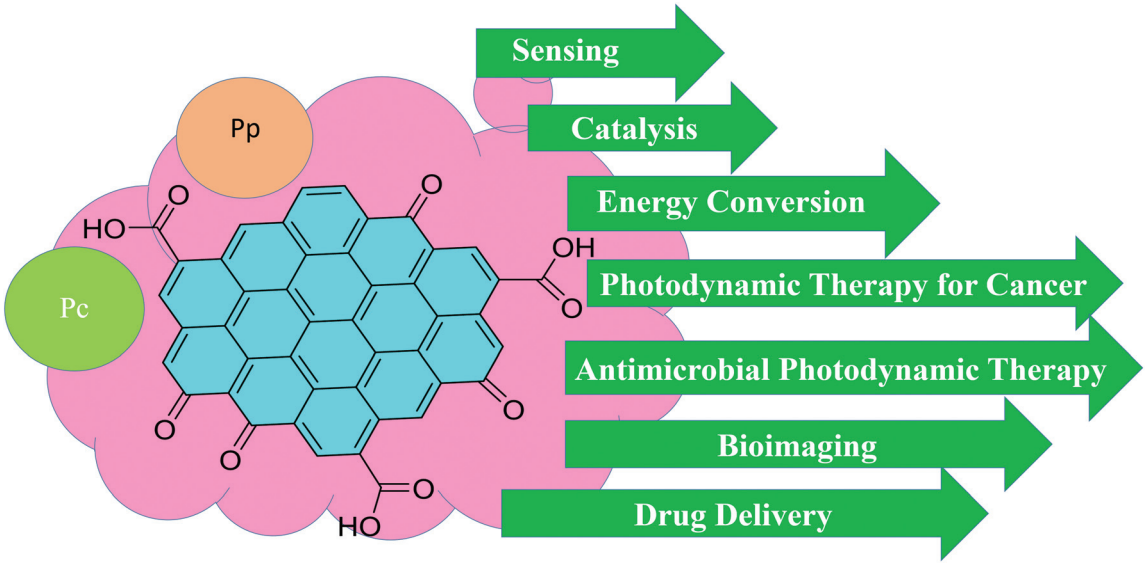

Fig. 5 Various applications of GQD-Pp/Pc conjugates.

data security, and sensing using a combined multi-technology approach[26] (Table 1).

4.1.1 Sensing of heavy metals. The success of the MPp collection culminated in the development of GQD-Pp/Pc hybrid systems as sensor arrays mostly based on the "turn-OF" principle, involving fluorescence quenching due to the inner filter effect (IFE) and FRET.[1,133,224,225] Field-effect transistor (FET)/IFE analysis is widely used to understand the sensing mechanism of GQD/porphyrin hybrid systems. IFE originates from the overlap of the absorption band of GQDs with the fluorescence excitation or emission spectrum of porphyrin. IFE is an effective tool in converting analytical absorption signals to fluorescence signals and provides better sensitivity and selectivity in complex biological conditions compared to other fluorescence quenching mechanisms such as photoinduced electron transfer (PET) and FRET. Another advantage of IEF-based sensors is that they do not require any covalent linkage between the receptor and fluorophore or surface modification of GQDs, thus providing simplicity and flexibility in the construction of probes. Zhang *et al.*, for the first time, demonstrated the catalytic effect of nitrogen-doped GQDs (N-GQDs) in the synthesis of MP-hybrids for the rapid sensing of Cd^{2+} ions, resulting in the fluorescence quenching of NGQDs due to the IFE of porphyrin on the assembled NGQDs.[212] Peng *et al.* demonstrated the rapid detection of Hg^{2+} ions due to the IFE of porphyrin on NGQDs. They reported that incorporation of Mn^{2+} ions in TMPyP was significantly faster in the presence of a trace amount of NGQDs and Hg^{2+}. The heavy metal Hg^{2+} deforms the structure of Pp, which facilitates the incorporation of the small divalent metal Mn^{2+} carried by the NGQDs (Fig. 6a). The formation of the metalloporphyrin resulted in a red shift in the absorption of the porphyrin and a quenching of its fluorescence due to the weakening of IFE.[213] This phenomenon was further used to monitor intracellular Hg^{2+} ions in lung cancer cells (A549) (Fig. 6b). Confocal imaging showed that TMPyP and NGQDs were cell permeable and individually gave red and blue fluorescence, respectively. However, when both TMPyP and NGQD were treated together, there was a quenching of the blue fluorescence, indicating that IFE can efficiently exist in the biological environment. Simultaneous treatment of TMPyP, Mn^{2+}, Hg^{2+}, and NGQDs showed quenching of the red fluorescence and remarkable enhancement in the blue fluorescence due to the formation of the Mn^{III}(TMPyP) complex under the synergistic effect of Hg^{2+}.[226] To date, the IFE of porphyrin in GQD/porphyrin conjugates has been exploited to detect heavy metal ions such as cadmium (Cd^{2+}) and mercury (Hg^{2+}) *via* the fluorescence "turn-OFF" approach. However, this approach suffers from low sensitivity and specificity, and interference from a variety of ligand or solvents may occur, leading to false signals.

4.1.2 Biosensing. A N-GQD-porphyrin hybrid was studied by Zhang *et al.* for sensing cadmium(II), which is one example of the use of this type hybrid of as a biosensor for fast and sensitive metal ion sensing.[212] The preferential recovery of fluorescence was observed by Monteiro *et al.* during the titration of a GO-Pp composite with guanine-quadruplexes (G-Q), which mimics a judicious "turn-off-on" biosensor for the detection of G-Q, presenting an opportunity for a better class of chemotherapeutics. Raman mapping was used for the first time to provide insight into stacking and electrostatic interactions.[219] Another *in vivo* application of GQD-Pp hybrids was proposed by Kamal *et al.* as an immunosensor for the detection of antigens of *Salmonella typhi* in human serum. Here, the structural assessment of the bio-mimetic Fe-porphyrin-GQD hybrid showed its bioimaging activity. This bioconjugated hybrid works as a prominent transfer system in the fluorescence system owing to its bio-conjugation sites and rich oxygen-containing surface.[220] A modified porphyrin and rGO

Table 1 Summary of the different types of GQD-Pp/Pc conjugate-based sensors

Sl. no.	Nanocomposite	Type of sensor	Target analytes	Phenomenon	Linear range	LOD	R^2	Sample	Ref.
1.	NGQD/TMPyP	Fluorescence probe	Cd^{2+}	Inner filter effect	0.5–8 μM	88.0 nM	—	Water	212
		UV-vis		Absorption	0.1–10 μM	90.0 nM	—		
2.	NGQD/TMPyP/Mn^{2+}	Fluorescence probe	Hg^{2+}	Inner Filter effect	0–100 nM	0.18 nM	—	Water	213
3.	GQD/FeTMPyP	Fluorescence Probe	H_2O_2	Inhibition of Inner Filter effect	2–300 μM	0.30 μM	0.993	Water	135
	GQD/FeTMPyP/GOx		Glucose		3–100 μM	0.50 μM	0.992	PBS/Water	
4.	M-GQD/TAPP	Fluorescence Probe	GSH	Switching OFF FRET ("turn ON")	0.67–130 nM	0.23 nM	0.999	PBS	1
			Cys		3.33–100 nM	1.30 nM	0.997		
5	M-GQD/ZnPc	Fluorescence Probe	Cys	Switching OFF FRET ("turn ON")	2–120 nM	0.85 nM	0.994	DMSO (25%)/PBS	214
			Hcys		1.5–120 nM	1.42 nM	—		
			GSH		5.0–150 nM	3.20 nM	—		
6.	GQD-T-ZnPc	Fluorescence Probe	Hg^{2+}	Fluorescence "turn ON"	0.1–20 nM	0.05 nM	—	DMF (25%)/PBS	203
	T-GQD-T-ZnPc				5.0–50 nM	24.7 nM	—		
7.	PEI-GQDs-Pc-Au@Ag	Fluorescence Probe	Hg^{2+}	Fluorescence "turn ON"	0.5–25.0 nM	0.25 nM	0.997	PBS	215
	PEI-GQDs/Pc-Au@Ag-Hg^{2+}		Cys	Fluorescence "turn OFF"	1.0–50 nM	0.72 nM	0.989		
			Hcys			0.87 nM			
			GSH			1.05 nM			
8.	CoPc-GQD	Gas Sensor	NO_2	Current Response	—	50 ppb	—	Air	216
9.	CoPc-HFIP-GQD CoPc–6FBPA–GQD	Gas Sensor	DMMP	Current Response	—	500 ppb		Air	217
10.	GQD@CoPc-COOH	Electrochemical or photoelectrochemical	Hydrazine	Electrocatalytic	—	8 μM	—	0.1 M NaOH	218
	GQD@CoPc-NH_2				—	43 μM	—		
11	GCE-GQD-CoPc (π–π)-aptamer	Electrochemical impedance spectroscopy (EIS)	Prostate specific antigen	Impedance	1.2–2.0 pM	3.66 pM		PBS	111
		Differential pulse voltammetry				0.66 pM			

hybrid was fabricated by Wang *et al.*, functioning as a biosensor for the rapid and selective DNA detection of *M. tuberculosis* and its resistant strands. As a result of its electrical and morphological characteristics, broad surface area, high electron transferability, and high loading efficiency for bioreceptors (covalently bonded) offered by its carboxyl functional groups, the biosensor exhibited excellent sensitivity towards the hybridization of DNA. Measurements using several independent biosensors were used to assess the reproducibility of this DNA hybridization platform.[221] Various studies using rGO-porphyrin and GQD-Pp composite have been reported for the electrochemical sensing of serotonin, dopamine, and glucose sensing, demonstrating enhanced selectivity and sensitivity towards these analytes.[222,223]

Zhang *et al.* developed a "turn-ON" fluorescence sensor *via* optical sensing for the detection of hydrogen peroxide (H_2O_2) and glucose using a GQD/FeTMPyP hybrid system (Fig. 6c). The absorption band of metalloporphyrin (FeTMPyP) has a complementary overlap with the emission band of GQDs, leading to fluorescence quenching of GQDs due to IFE. The reversibility of the fluorescence of GQD *via* the hindrance of IFE permits the detection of glucose and H_2O_2. Thus, designed MPs exhibit potential to be highly inventive for other desirable analytes.[135] Similarly, Xue *et al.* developed rapid, sensitive, and selective "turn-ON" fluorescent probes for the detection of biothiol (GSH or cystine) in a FRET system *via* the Michael addition reaction between maleimide-functionalized GQDs (M-GQDs) and tetrakis(4-aminophenyl) porphyrin (TAPP). The hybrid system is formed *via* stacking and electrostatic interactions between the negatively charged GQDs (due to the presence of carboxylate group on their surface) and positively charged porphyrin (due to the presence of amine group on its surface), which results in fluorescence quenching of M-GQDs by porphyrin due to FRET. In contrast to the single component detection system, the hybrid-based FRET system exhibited rapid, selective, and sensitive detection[302] in a wider range without interference from other biomolecules in the quantitative spotting of biothiol.[1] This hybrid system was used for detection of biothiol (GSH) in blood serum and fruits, with detection recoveries ranging from 95% to 106% and an relative standard deviation (RSD) less than 2%. Similarly, Achadu *et al.* reported the detection of biothiol using an M-GQD and zinc phthalocyanine (ZnPc) hybrid system.[214] Another interesting report by Achadu *et al.* demonstrated a novel supramolecular

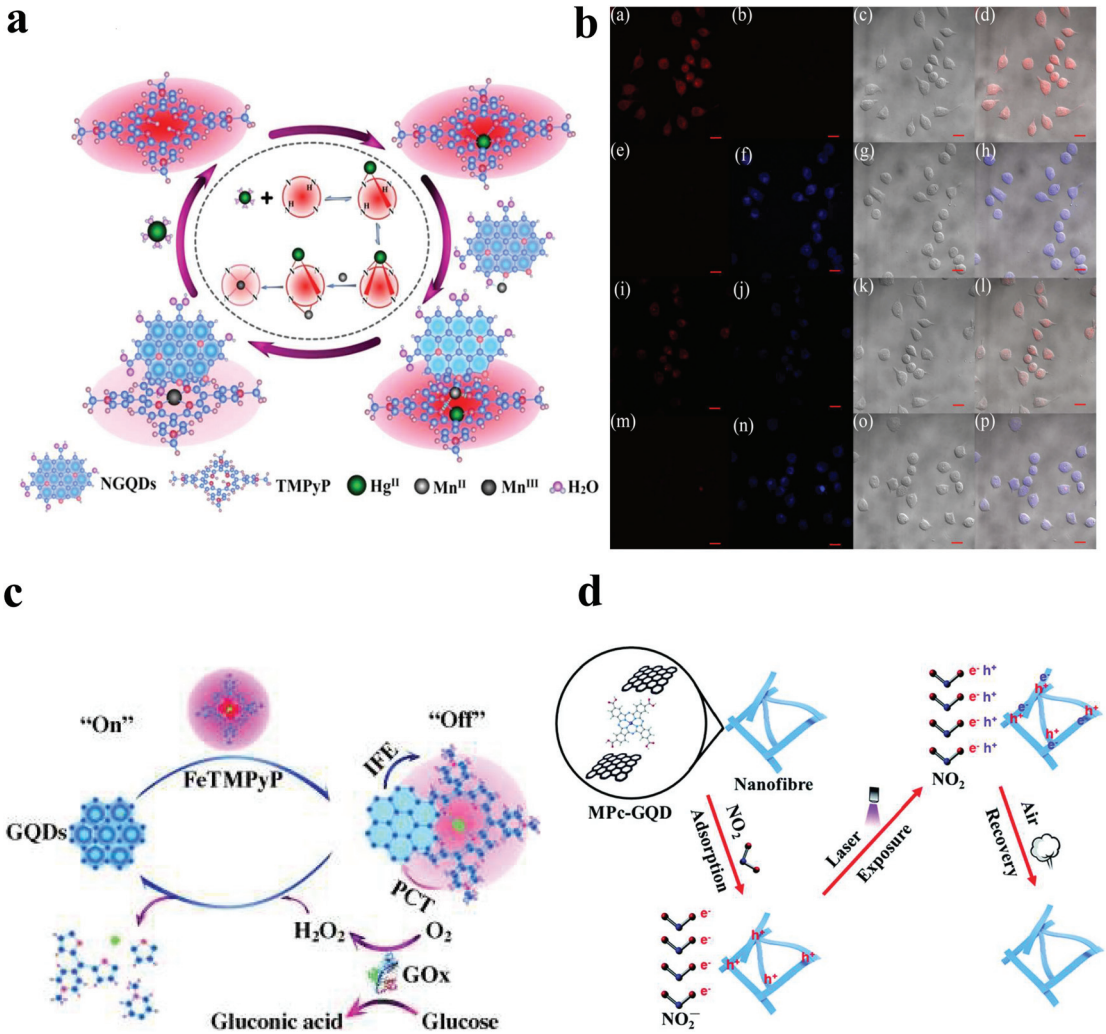

Fig. 6 (a) Schematic showing the synergistic mechanism of NGQDs and Hg^{2+} in the co-ordination of Mg^{2+} with TMPyP. (b) Confocal microscopy images of lung carcinoma cells (A549). First column shows images obtained through the red channel, second column is the green channel, third column is the bright field, and the fourth column is the merged image. Panel (a–d) cells treated with TMPyP; panel (e–h) cells treated with NGQDs; panel (i–l) cells treated with TMPyP and NGQDs; and panel (m–p) cells treated with TMPyP, NGQDs, Hg^{2+} and Mg^{2+}. Reprinted with permission from ref. 226 Copyright 2018, ACS. (c) Schematic showing the sensing of H_2O_2 and glucose through the inhibition of IFE between GQDs and TMPyP. Reprinted with permission from ref. 227 Copyright 2015, Wiley-VCH Verlag GmbH & Co. KGaA, Weinheim. (d) Schematic diagram showing the adsorption and desorption of NO_2 on MPc/GQDs. Reprinted with permission from ref. 216 Copyright 2021, RSC.

hybrid system consisting of polyethylenimine (PEI)-GQD and mercaptopyridine-substituted zinc phthalocyanine (Pc)-Au@Ag nano-alloys using "OFF–ON–OFF" fluorescence for the detection of Hg^{2+} and biothiol in an aqueous medium. This strategy is based on turning "ON" the quenched fluorescence of the PEI-GQD-Pc-Au@Ag hybrid system in the presence of Hg^{2+} and switching "OFF" the fluorescence in the presence of biothiol due to the stronger affinity between Hg^{2+} and biothiols and the formation of a strong Hg–S bond. These nanoprobes were target selective and highly stable in the presence of other molecules, exhibiting their successful application.[215]

4.1.3 Gas sensing by GQD-Pc conjugates. Presently, GQD-Pp/Pc conjugates provide an ideal avenue for the fabrication of wearable sensors. In 2021, Jiang *et al.* described how the surface of metal phthalocyanine (CoPc) nanofibers was anchored by GQDs for sensing NO_2. The gas sensitivity performance was greatly enhanced due to the formation of charge transfer conjugates at room temperature compared to the individual material. The introduction of GQDs provides good conductivity to CoPc, and thus fastens the response of the hybrid material. The authors suggested the mechanism of NO_2 sensing by the conjugate, wherein NO_2 accepts an electron from the conjugate and transforms into NO_2^-. The holes formed in the hybrid system change the conductivity of the sensor, with a lower detection limit. Thus, the reproducibility, selectivity, and stability of the hybrid materials are greatly improved (Fig. 6d).[216] Due to the unique features of reproducibility, selectivity, and stability of the MPc/GQD hybrid system as a gas sensor, the same group used a similar system for the detection of dimethyl methylphosphonate (DMMP). The

hybrid system showed a good gas response for the detection of DMMP due to the presence of a strong hydrogen bond between hexafluoroisopropanol (HFIP) and hexafluorbisphenol A (6FBPA) conjugated to MPc and DMMP. The presence of GQDs in the hybrid system increased the conductivity of the Pc derivative, and thereby fastened its sensing response.[217]

4.1.4 Electrochemical sensing by GQD-Pc conjugates. The literature shows that GQDs are a great platform for the specific and sensitive recognition of biomarkers, which are highly synergistic with electrochemical sensors.[303] Recently Nxele *et al.* developed an aptasensor for the electrochemical detection of the prostate specific antigen (PSA) using different combinations of aptamer, CoPc, and GQD modified on a glass carbon electrode (GCS). The best efficacy was obtained by the GCE-GQD-CoPc (π–π)-aptamer with an LOD of 3.66 pM determined by electrochemical impedance spectroscopy (EIS) and 0.66 pM by differential pulse voltammetry (DPV). The LOD is much lower than the cut off value of PSA, *i.e.*, 13.3 nM, for a patient with prostate cancer. The electrode showed specificity towards PSA even in the presence of interfering biological molecules such as BSA, glucose and L-cysteine. The aptasensor showed good stability, reproducibility, and repeatability.[228] Centane *et al.* explored the electrochemical properties of Pc conjugated with electron-withdrawing groups (–COOH) and electron-donating group ($–NH_2$) when non-covalently anchored to π-electron-rich graphene quantum dots. The incorporation of GQDs in amino conjugated Pc (GQD@Pc-NH_2) resulted in a lower potential compared to only Pc-NH_2. In contrast, when GQDs were conjugated to Pc functionalized with an electron-withdrawing group such as carboxy (GQD@Pc-COOH), the hybrid demonstrated a higher hydrazine oxidation potential than Pc-COOH. Nevertheless, GQD@Pc-COOH showed a better catalytic current than GQD@Pc-NH_2. The good catalytic activity is governed by both the decrease in potential and increase in current. Hence, the catalytic current for GQD@Pc-COOH dramatically increased compared to that of Pc-COOH and GQD@Pc-NH_2, resulting in a better LOD for the detection of hydrazine compared to GQD@Pc-NH_2.[218]

4.2 Energy conversion

4.2.1 Light-harvesting antenna (LHA). Various challenges are involved in designing artificial LHAs that work well in aqueous solution through a regular combination of multi-donor and single acceptor structures with efficient energy transfer capability. The hybrids of GQDs and porphyrin provide an excellent electron donor and acceptor pair, whereas porphyrin and its derivatives also behave as natural or artificial LHAs. However, the absorption spectrum of porphyrin only covers a limited portion of the visible region, which is the biggest hurdle for light harvesting. As mentioned earlier, GQDs have a broad absorption spectrum with a high extinction coefficient, and thus the light-harvesting property of porphyrin can be easily enhanced by using GQDs as donors. Accordingly, Liu *et al.* reported novel aqueous LHAs with the srikaya-like structure of multiple GQDs as donors and a single porphyrin unimolecular micelle as an acceptor. This construct overcame the problems related to the insolubility of porphyrin, minimized the electron transfer, and maximized the energy transfer efficacy from the GQD donor to the porphyrin acceptor by up to 93.6% with an antenna effect of 7.3 in aqueous solution[233] (Fig. 7a).

4.2.2 Solar cells. Solar cells or photovoltaic cells have the ability to transform light energy into electricity due to the photoelectric effect. GQDs due to their large Bohr exciton radius and 0D quantum confinement effect, can be used to tune the HOMO–LUMO gap over a wide spectrum range (ultraviolet to visible to infrared wavelength) by varying their size, having implications in solar cells. However, the low photoluminescence quantum yield (below 20%) of pristine GQDs and their absorbance band in the UV region hinder their effective utilization as a photosensitizer in dye-sensitized solar cells (DSSCs). Accordingly, doping GQDs with heteroatoms (S, F, B, and N) provides them with tunable photoluminescence and band gap energy in the visible region for better application in solar cells. Compared to GQDs, N-doped carbon quantum dots (NCQDs) show relatively better performance with TiO_2, exhibiting an efficiency of 0.13%.[234] This efficiency is further enhanced in the presence of conventional dyes such as N3 and N719 as a co-sensitizer, *e.g.*, (NGQDs-N719)/TiO_2 and NFS-GQDs-TiO_2-N719 having a power conversion efficiency (PCE) of 7.49% and 11.7%, respectively (Table 2). In DSSCs, N719, which is a ruthenium compound, is widely used as a photosensitizer, but it suffers from several disadvantages such as multi-step synthesis, problems in purification and use of expensive material.[235] Thus, to overcome this, a metal-free organic photosensitizer, *i.e.*, porphyrin, has emerged as an alternative due to its to high visible extinction coefficient, 2D π-electron framework, excellent light-harvesting properties (mimicking natural photosynthesis) and tunable functional molecule for optoelectric applications, especially in DSSC.[236,237] Furthermore, the poor performance of porphyrin[238] due to aggregation can be overcome by synthesizing nanohybrids, wherein porphyrin is co-sensitized with GQDs. The presence of GQDs improves the electron movement and reduces the charge recombination, increasing the performance of solar cells.[239] Mandal *et al.* demonstrated that smaller-size GQD/porphyrin nanohybrids showed type-II band energy alignment, where their LUMO (on GQD) and HOMO (porphyrin) had larger spatial charge separation, resulting in the low recombination of electron–hole pairs to increase the photovoltaic cell efficacy. In contrast, larger-size GQDs in the nanocomposite showed type-I band energy alignment, where the HOMO and LUMO were located on the GQDs, resulting in less charge separation. However, larger nanohybrids can be converted to type-II band alignment by functionalizing Pp with an electron-donating group such as $–NH_2$ or $–OCH_3$. Another interesting feature was evident from the density of state (DOS) studies on nanocomposites, where the energy gap between the LUMO of GQDs and Pp controls the rate of electron transfer from the photoexcited Pp to GQDs, which increases with an increase in the size of GQDs.[42,57,240,241] Furthermore, Sehgal *et al.* fabricated a porphyrin sensitized solar cell (PSSC),

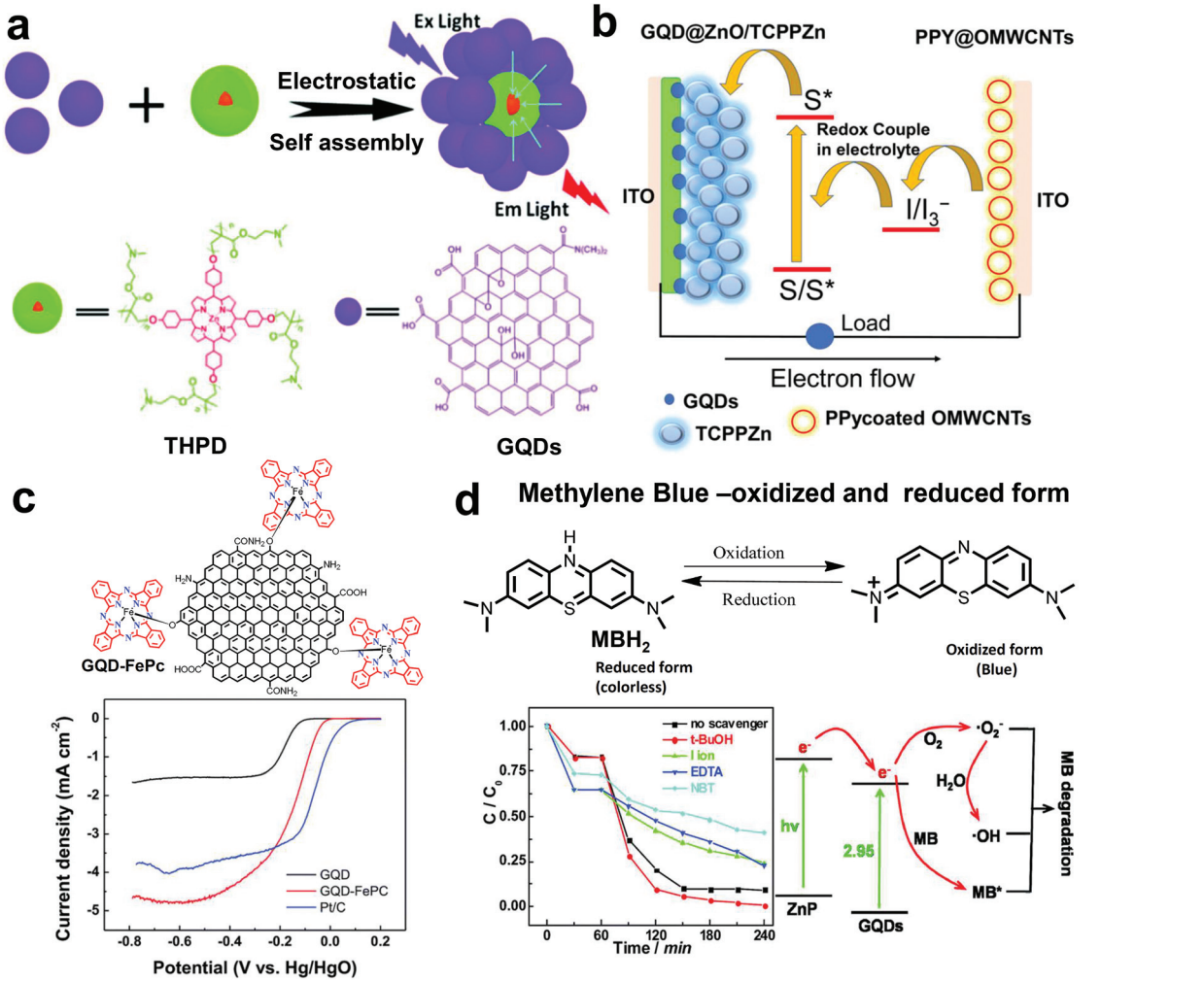

Fig. 7 (a) Schematic diagram showing the light harvesting antenna (LHA) nanosystem with multiple GQD donors and a single porphyrin unimolecular micelle as the acceptor formed through electrostatic self-assembly. Reprinted with permission from ref. 229 Copyright 2016, RSC. (b) Diagram showing the schematic energy transfer mechanism of the GQD@ZnO@TCPPZn nanocomposite in the fabricated porphyrin sensitized solar cell (PSSC). Reprinted with permission from ref. 230 Copyright 2018, Elsevier B.V. (c) Linear sweep voltammetry (LSV) of GQD-FePc. Reprinted with permission from ref. 231 Copyright 2017, RSC. (d) Effect of no scavenger, *tert*-butyl alcohol, iodide ion, EDTA and NBT on the degradation of methylene blue by the GQD–Zn porphyrin under xenon lamp irradiation. (Right) Schematic of the photocatalytic process for the GQD–Zn porphyrin under visible light. Reprinted with permission from ref. 232 Copyright 2015, RSC.

GQD@ZnO/TCCPPZn, where GQD@ZnO acted as the photoanode and zinc tetrakis(4-carboxy phenyl) porphyrin (TCPPZn) as a sensitizer (Fig. 7b). The enhancement in the photovoltaic properties was due to the ability of GQDs to emit multiple excitons from a single photon[242] and transfer them into the conduction band (CB) of ZnO and the mechanism of electron transfer occurred through electron injection from GQDs to ZnO. Therefore, this type of hybrid composite device holds great potential for application in dye-sensitized solar cells (DSSC) and PSSCs at an economical low cost.[230]

4.3 GQD/Pp and GQD/Pc as catalysts

4.3.1 Electrocatalysis. GQDs can serve as an efficient alternatives to platinum-based electrocatalysts for the oxygen reduction reaction (ORR) given that GQD can lower the oxygen adsorption barrier and first electron transfer barrier, thereby providing enhanced electrocatalytic activity for the ORR due to the increase in electrocatalytically active edge sites. Doping of GQDs with nitrogen (N-GQDs) is highly beneficial for the enhancement of their electrocatalytic activity for the ORR. N-GQDs increase the charge density of graphene, which results in the better affinity of oxygen with graphene, and thus weakens the O–O bonding on the surface of the catalyst, indicating reduced overpotential and better electrocatalytic activity for the ORR[250,251] (Table 3). However, some hurdles associated with GQD, such as low limiting current density and onset potential, still exist. Metallophthalocyanine (MPc) and metalloporphyrin (MPp) are known for their electrocatalytic properties, but their use is limited due to their low conductivity, which affects their electron transfer and electrochemical

Table 2 *J–V* characteristics of GQDs, doped GQDs and GQD-MPc/MPp as photoanodes

SL. no.		Photocurrent density at short circuit voltage (J_{sc}) (mA cm^{-2})	Open circuit voltage (V_{oc}) (V)	Fill factor (FF)	Efficiency η (%)	Ref.
1.	NGQDs/ZnO nanorods	0.92	0.34	—	0.121	243
2.	ZnO nanowires-GQDs	0.45	0.8	0.5	0.2	244
3	SNGQD/C-ZnO NT	3.4	0.45	—	0.59	245
4	ZnTCPP (12 h)/N719 (a ruthenium complex)	18.9	0.61	0.55	6.35	246
5	NGQD/TiO_2	1.49	0.48	0.53	0.37	247
	N719/TiO_2	12.61	0.71	0.64	5.7	
	(NGQDs-N719)/TiO_2	17.65	0.72	0.59	7.49	
6.	NFS-GQD-TiO_2	0.35	0.51	0.53	0.71	248
	NFS-GQDs-TiO_2-N719 dye	22.6	0.79	0.7	11.7	
7	DNA-ZnO Nano flower + B-GQDs/ N719	—	—	—	3.7	249
8	ZnO@TCPPZn	7.2	0.37	0.307	0.817	230
	GQD@ZnO@TCPPZn (30%)	8.9	0.47	0.400	1.67	
	GQD@ZnO@TCPPZn (40%)	10.1	0.48	0.507	2.45	
	GQD@ZnO@TCPPZn (50%)	9.8	0.48	0.4377	2.05	

Table 3 Electrochemical parameters for the catalytic oxygen reduction reaction (ORR)

SL. no.	Type of electrode	ORR onset potential (V)	Limiting current (mA cm^{-2})	No. of electrons followed for ORR	Ref.
1	N-Colloidal GQD	−0.1	—	4-Electron pathway	251
2	N-GQD/graphene (N/C atomic ratio of 4.3%)	−0.16	—	4-Electron pathway	250
3	N-GQDs-35-10/graphene	−0.11	—	4-Electron pathway	256
4.	FePc/MWCNTs	−0.09	−4.5	4-Electron pathway	254
	Pt/C	−0.03	−4.7	4-Electron pathway	
5.	(G-dye-Fe-Porphyrin)$_n$ MOF	−0.087	—	4-Electron pathway	257
6	GQDs	−0.13	−4.68	2-Electron pathway	231
	GQD–FePc	−0.04	−1.65	4-Electron pathway	

activity.[252,253] Therefore, the catalytic activity of FePc supported on muti-walled carbon nanotubes (FePc/MWCNT) has been studied for the oxygen reduction reaction, which was found to be comparable to that of the commonly used Pt/C catalyst with similar current densities and a very low overpotential (60 mV).[254]

Therefore, conjugating MPc/porphyrin with N-GQDs will be a potential candidate for a synergistic effect in electrochemical reactions. The functionalization of MPc/porphyrin with N-GQDs containing pyrrolic nitrogen atoms provides additional nitrogen atoms to GQDs, modifying the bandgap, leading to faster charge transfer and synergistically enhancing the electrocatalytic activity performance of GQDs, while averting the aggregation of FePc (Fig. 7c). The results demonstrated an amended onset potential, remarkable methanol tolerance, a higher limiting current density compared to Pt/C, and electrochemical stability without CO poisoning for the hybrid system, which may have further commercial application in fuel cells.[94,103] Pham *et al.* studied the thermodynamic and kinetic aspects of FePc and FePc-GQD and their catalytic activities, and concomitantly their tolerance toward CO through density functional theory (DFT) calculations. They showed that the four-electron pathway is the most energetically favourable for the ORR in both cases. FePc-GQD showed high catalytic ORR activity, with a limiting potential of 0.70 V, which is comparable to that of Pt/C (0.79 V). FePc-GQD showed high CO tolerance due to its positive CO adsorption energy of 2.39 eV, unlike the FePc system. Thus, all these characteristics make FePc-GQD an efficient electrocatalyst for the ORR, which can be used for commercial application in fuel cells.[255] Reduced GQDs (rGQD) show better electrocatalytic activity than amino-functionalized GQDs given that the reduction process involves the elimination of carboxyl, epoxy, and hydroxy groups on the surface of GQDs, which results in narrowing of the energy band gap of GQDs, thus enhancing electron transfer properties.[252] Centane *et al.* conjugated rGQD covalently and non-covalently with cobalt phthalocyanine (CoPc), where CoPc has three *tert*-butyl substituents, acting as electron donating groups (push), and a single COOH as an electron-withdrawing group (pull). These push–pull substituents enhance the electron delocalization, which leads to facile electron transfer properties in CoPc. The rGQD-CoPc conjugates were used for the electrocatalysis of hydrazine oxidation on a glassy carbon electrode and improved catalytic behavior was obtained in the non-covalently (π stacking) conjugated CoPc compared to the covalently conjugated CoPc, giving an LOD of 2.1 μM and 4.4 μM, respectively.[252]

4.3.2 Photocatalysis. The synergistic and cooperative effects between macrocycles and GQDs in close proximity have tremendous influence in governing their physicochemical properties *via* bond activation, catalysis, reactivity, *etc*.[258,304] Metalloporphyrin or porphyrin derivatives have a high extinction coefficient in visible light and can generate a good quantum yield of singlet oxygen upon photoexcitation. This property has applications in various photocatalytic processes, especially in oxidation reactions.[143] However, homogeneous catalysis has various disadvantages such as difficult recovery and reuse of the catalyst, and additionally the catalyst suffers from intermolecular self-oxidation, dimerization and decomposition during the reaction, together with high preparation cost. These problems can be easily overcome by immobilizing porphyrin on a solid surface. GQDs can provide good support given that they have a large surface area for loading, excellent electrical and optical properties, uniform dispersion in water, and photostability.[259] Lu *et al.* demonstrated the photocatalytic degradation of an organic pollutant under visible-light irradiation using zinc porphyrin-functionalized GQDs (GQDs/ZnP) (Fig. 7d). The mechanistic investigation suggested that the superoxide radical ($^{\bullet}O_2^-$) and holes (h_{VB}^+) were involved in the photocatalytic reaction. Doping of GQDs with electron-rich atoms such as N and S lower their bandgap, resulting in a broad absorbance band in the visible region. Therefore, S, N: GQDs as photocatalytic carriers improve the energy conversion of solar light for aerobic oxidation reactions due to their broad visible light absorption.[232]

Mahyari *et al.* synthesized efficient, green and visible-light recoverable photocatalysts using anionic Fe(III)tetra(4-sulfonatophenyl) porphyrins (FeTSPP) supported on S, N: GQDs for the selective aerobic oxidation of alcohols to the corresponding carbonyl compounds.[260] The same group synthesized cobalt porphyrin-supported nitrogen and phosphorus co-doped graphene quantum dots/graphene for the aerobic oxidation of alcohol with a much higher conversion (~92%) and selectivity (~86%) than most of the reported photocatalysts. The high photocatalytic activity under mild conditions, reusability, and selectivity of CoTSPP@N,P:GQDs/G make them potential materials for using solar light for energy conversion and environmental therapy.[261] Notably, the doping of GQDs with nitrogen induces ionic interactions between the active sites of porphyrin (TSPP) and the support, which increases the hydrophilic character of the catalyst, and consequently increases the dispersion and stability of the catalyst in aqueous solution.[262]

4.4 Therapeutic applications of GQD and Pp/Pc hybrid systems

Porphyrin, due to its abundant presence in nature and its physiological properties, has become an attractive candidate in the field of therapeutics. This is a crucial topic because porphyrin-based nanostructures can help to identify cancer and other degenerative diseases that are difficult to detect or cure in the early stage. This review sheds light on GQD Pp/Pc hybrid systems, their interactions, and applications spanning the theragnostic role of Pp/Pc in biomimetic systems. Porphyrins and their analogous macrocycles display fascinating, photochemical, and luminescence properties besides disease diagnosis, sensing, therapy, and biomedical applications, indicating their high prospects in the treatment of numerous diseases.[252,261,263] Various Pp derivatives serve as a chemical basis for many drugs that are in preclinical and clinical trials.[264]

For instance, the application of PDT and antimicrobial/antiparasitic PDT is of prime importance.[3,265] Carbon nanomaterials offer competent schemes to augment the bioavailability and integrate targeted delivery features in traditional pharmaceuticals, enhancing their efficiency and reducing their toxicity, thus improving the therapeutic effect. The previously mentioned hurdles can be overcome as follows: (1) amalgamation of hydrophilic groups in the porphyrin ring, while governing the interaction with living systems and (2) integration into nanovehicles and delivery nanosystems. Unquestionably, nanohybrid systems are the current choice to expand the transport and tumor targeting efficacy. Furthermore, formulations that embrace the viewpoint of combined therapy and image guidance are valuable to improve the clinical outcome. Currently, the "one-for-all" concept is gaining support in the field of photonanomedicines, where it overcomes the limitations concerning multistep fabrication and low reagent loading of traditional delivery systems based on various nanoparticles.[266]

In 2015, Su *et al.* first synthesized porphyrin-functionalized graphene oxide for the photothermal ablation of the glioblastoma cell line U87-MG using 808 nm irradiation.[267] The findings pave the way for the therapeutic use of graphene nanosheets in cancer treatment, particularly for deep-seated tumors. In continuation of this research, in 2016 the same group synthesized L-arginyl-glycyl-L-aspartic (RGD) conjugated Pp immobilized nano-graphene oxide (PNG) to selectively target brain cancer cells with improved clinical effectiveness and no discernible side effects. The proficient photothermal transformation of PNG-RGD, as well as its ligand-targeting activities inhibited tumor development in mice upon laser irradiation, whereas tumour recurrence was observed in the case of graphene oxide (GO). Thus, PNG-RGD can be a potential photothermal therapy (PTT) agent for the therapy of brain tumors, with active photo-to-thermal transfer and a high penetration depth in tissues.[259] In 2018, Santos *et al.* synthesized nano-GO covalently linked to glycol porphyrins and studied the biocompatibility of the hybrid system with human Saos-2 osteoblasts. Their proliferation, viability, and ROS generation findings showed that the graphene-based hybrid nanomaterials exhibited excellent biocompatibility, making them very promising for use in biomedicine, especially in cancer therapy.[24] However, despite these recent advancements, GO still has some limitations and challenges, including the lack of reproducibility in its synthesis, which may weaken its final physicochemical properties and workability.[27] Thus, to overcome a few of the aforementioned challenges, Xu and colleagues were the first to develop an organic-solution-processable functionalized-graphene (SPFgraphene) hybrid material

with Pp with rich photophysical properties, together with optical-limiting properties, which is largely due to greater photoinduced electron- and/or energy-transfer processes.[165] Given that graphene is a good electron acceptor, the energy/electron transfer can be easily modulated by non-covalently or covalently conjugating electron-donating organic moieties such as Pp/Pc.[268] Suhag *et al.* synthesized Pp-functionalized nitrogen-doped graphene nanosheets (PFNGS) for the detection of nitric oxide (NO) released from macrophage cells. PFNGS were biocompatible, facile, highly sensitive, and possessed exceptional electrocatalytic properties, together with reproducibility and stability. The *in vitro* studies of PFNGS in murine macrophage cells showed that they were cytocompatible with 96% cell viability. Furthermore, the blood compatibility studies demonstrated that PFNGS were hemocompatible.[269]

Due to their versatile properties, GQDs can be extensively used in a variety of biological applications such as nanomedicine (*e.g.*, drug delivery), bio-sensing, and bio-imaging. However, it is important to determine the cellular uptake, circulation, and cytotoxicity of unmodified GQDs, functionalized GQDs, and doped GQDs before their use as conjugating materials. Various parameters such as concentration, chemical doping, methods of synthesis, particle size, and surface functionalization govern the uptake mechanism of GQDs inside cells and their toxicity.[266,270,271] GQDs can be internalized through caveolae-mediated endocytosis and are partially involved in the energy-dependent endocytosis pathway in human gastric cancer (MGC-803) and breast cancer (MCF-7) cells. In addition, it has been reported that nanometer-sized GQDs are less toxic compared to micrometer-sized graphene oxide (GO) based on different biological studies such as intracellular ROS level, cell viability, mitochondrial membrane potential, and cell cycles. The toxicity of GO is a consequence of the change in the cell membrane integrity, resulting in the hemolysis of cells, which is not the case with GQDs.[266]

GQD-Pp/Pc-based hybrid systems with more favorable photophysical properties can serve as third-generation PSs. GQD-porphyrin/Pcs hybrid systems can generate a high quantum yield of ROS, mainly singlet oxygen, upon light irradiation, exhibiting great potential for enhanced PDT and PTT combined therapy in both *in vitro* and *in vivo* models.[272,273] The suitable design of GQD-Pp/Pc hybrid systems can solve problems related to their synthesis, including the size mismatch problem between GQDs and porphyrin and the insolubility of porphyrin in water, and also increase their light absorption range, increasing the energy transfer efficiency from GQD donors to porphyrin acceptors and their potential tumor targeting ability by grafting certain tumor-targeting groups.[140] According to Gao *et al.*, the fluorescence efficiency of Pp increased when titrated with varying concentrations of GQDs. The fluorescence emission of Pp was efficiently improved by the GQDs due to FRET, which is an advantage in biosensing and bioimaging. These studies also shed light on GQD and porphyrin host–guest nanoensembles, which are important for exploiting the synergistic properties of Pp/Pc and GQDs in drug delivery, bioimaging, and developing novel PDT agents that outperform other traditional agents in terms of water dispersibility, singlet oxygen generation, and biocompatibility.[124,274,275]

4.4.1 Photodynamic cancer therapy. Pp-based derivatives have been extensively used as PSs for PDT in cancer treatment, being noninvasive[276] in nature. PDT leads to the production of ROS in the tissue, which offers a promising modality for tumor destruction.[296] PSs play a central role in PDT, which produce cytotoxic ROS to abolish tumor cells *via* apoptosis/necrosis upon exposure to an appropriate wavelength of light.[151,277] An ideal PS for PDT should have low dark toxicity, solubility in bodily fluids, photochemical reactivity with high triplet state yields, and a long triplet state lifetime.[119] Given that Pp/Pc molecules possess multiple intrinsic theragnostic features, these molecules have enormous virtues for cancer treatment. Porphyrin molecules absorb light energy to transform it into potent therapeutic properties, where light energy interacts with surrounding oxygen to generate ROS. Pp/Pc endow excellent PDT effects, being highly energized and toxic in nature. Besides, these molecules have the ability to generate hyperthermia using photon energy released as molecular vibration, which culminates in a photothermal therapeutic (PTT) effect[55,278–280] (Fig. 8a).

PTT uses nanoporphyrins as multiphase nanotransducers to convert light to heat inside tumors, while PDT uses nanoporphyrins to convert light to singlet oxygen.[69] Several Pp derivatives and molecular PS were investigated with the aim to overcome significant problems such as reduced aqueous solubility, dark toxicity, restricted structural stability, and short excitation wavelength arising due to scattering or absorption by tissues. Tetrapyrrole-based derivatives are the most commonly applied PS in the PDT domain due to their structural characteristics, low toxicity, and ability to generate a high quantum yield of superoxide anion, singlet oxygen, hydroxyl radicals, and hydrogen peroxide.[281] Generally, the features of these chromophores include a relatively long lifetime and high triplet quantum yield, which promote the creation of $^1O_2$ in high quantum yield, intense absorption within the optical therapeutic window ranging from 650 nm to 850 nm with better penetration depth and minimum absorption and scattering, together with the absence of dark toxicity.[187,282–284]

A recent strategy to tackle important issues consists of mimicking nature using biologically inspired hybrids, namely porphyrinoid-based photosensitizes (PSs),[305] which have been classified into three groups. First-generation Pp PSs include hematoporphyrin derivatives and Photofrin, which have been used for the treatment of skin cancer and colorectal cancer. However, their use is restricted owing to their chemical impurity, poor extinction coefficient and low water solubility, prolonged skin photosensitization, short circulation time in the blood, and suboptimal tissue penetration. Porphyrin-based derivatives have developed into second-generation PS for PDT in cancer treatment. Second-generation porphyrin PSs (*e.g.*, Lutrin) alleviate the problems of first-generation PSs but have high toxicity, low cellular uptake, and poor light penetration. Eventually, third-generation porphyrin PSs refer to modifi-

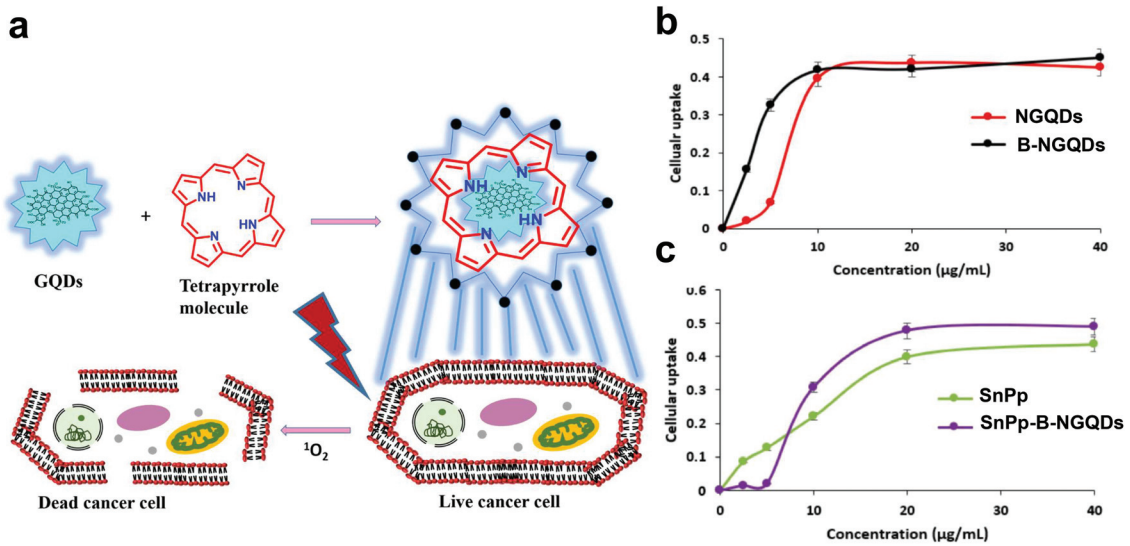

Fig. 8 (a) PDT for innovative cancer therapy (b and c) Cellular uptake of NGQDs, SnPp, and SnPp-B-NGQD in MCF-7 cells at various concentrations over 24 h. Reprinted with permission from ref. 192 Copyright 2021, Elsevier Ltd.

cations of second-generation PSs such as porphyrin or its derivatives conjugated to site-specific delivery agents and/or formulated with nanocarriers (*e.g.*, modified porphyrin with GQDs)[305] or targeting antibodies or nanoparticles to increase their cellular uptake at the target site *via* improved characteristics, such as less aggregation, better solubility in physiological media and selective accumulation in the targeted tissue.[13,60,125,126] Menilli *et al.* discovered that cationic porphyrins are more easily internalized than their non-cationic counterparts, and their positively charged structures allow non-covalent bonding with both GQDs and GO at physiological pH.[119]

Most organic PS systems, including third-generation PS and porphyrin derivatives, are hydrophobic in nature, resulting in limited biocompatibility and unspecific tissue accumulation, especially when not appropriately adorned with immunosuppressing moieties and targeting labels. Consequently, they are more prone to aggregation, which compromises the therapeutic efficacy of the drug, leading to lower singlet oxygen generation and poor fluorescence in the aggregated state. Besides, nonselective activation or nonspecific drug leakage during blood circulation can lead to unwanted side effects such as toxicity and drug resistance.[8,151,285,286]

Unfortunately, most tetrapyrrole-based PSs are hydrophobic, creating masses in aqueous solutions, which prevent their biodistribution and even cause fluorescence self-quenching, prompting researchers to focus their efforts on Pp-nanomaterial-coupled systems.[18] GQD-porphyrin/Pc-based hybrid systems with more favourable photophysical properties can serve as third-generation PSs. The introduction of GQDs with Pp derivatives is an operative strategy to produce hydrophilic porphyrins, which are imperative for biomedical applications, including PDT.

In addition, GQD-Pp/Pc hybrid systems can generate a high quantum yield of ROS, mainly singlet oxygen, upon light irradiation, exhibiting great potential for improved PDT and PTT combined therapy in both *in vitro* and *in vivo* models.[273,289] Therefore, Cao *et al.* synthesized a multifunctional theranostic platform coupling polyethylene glycol (PEG) ylated and aptamer-functionalized GQDs loaded with porphyrin derivatives (GQD-PEG-P). Most importantly, GQD-PEG-P exhibited a PTT conversion efficiency of 28.58% and a high ϕ_Δ of 1.08, which enabled it to show a combined PTT and PDT effect for treating cancer. The *in vitro* MTT assay performed on non-small cell lung cancer (A549) cells showed significant cell death when irradiated simultaneously with a 635 nm and 980 nm laser. The GQD-PEG-P theranostic platform has significant biomedical potential because it combines therapeutics with effective cancer cell diagnostics[276] (Fig. 9a and b). Under white light, the novel hybrids GQD_1A and GQD_1B were tested by Santos *et al.* as phototherapeutic agents in a high-intensity breast cancer cell line (T-47D), and a significant photocytotoxic effect was seen at 10 nM. When compared to non-immobilized porphyrin, the coupling of GQDs to amino-porphyrin improved their effective cellular uptake in T-47D cells[18] (Fig. 9c). Magaela *et al.* studied the PDT effect of an Sn (IV) porphyrin linked with biotin-decorated nitrogen-doped graphene quantum dot nanohybrid, (SnPp/B-NGQD). Consequently, ϕ_Δ of 0.59 and 0.79 were achieved for SnPp and the SnPp-B-NGQDs, respectively, in DMSO. Studies showed that SnPp-B-NGQDs had greater cellular uptake, which correlates with its PDT activity against MCF-7 cells. SnPp-B-NGQDs showed high phototoxicity with an IC_{50} value of 10.4 μg mL^{-1} compared to SnPp alone with an IC_{50} value of 11.2 μg mL^{-1}, which implies that the biotin-decorated nitrogen-doped graphene quantum enhanced the activity of SnPp[192] (Fig. 8b and c). Managa *et al.* studied the PDT effect of a GQD/porphyrin nanocomposite in MCF-7 breast cancer cells. The nanoconjugates did not show any dark toxicity even at a high concen-

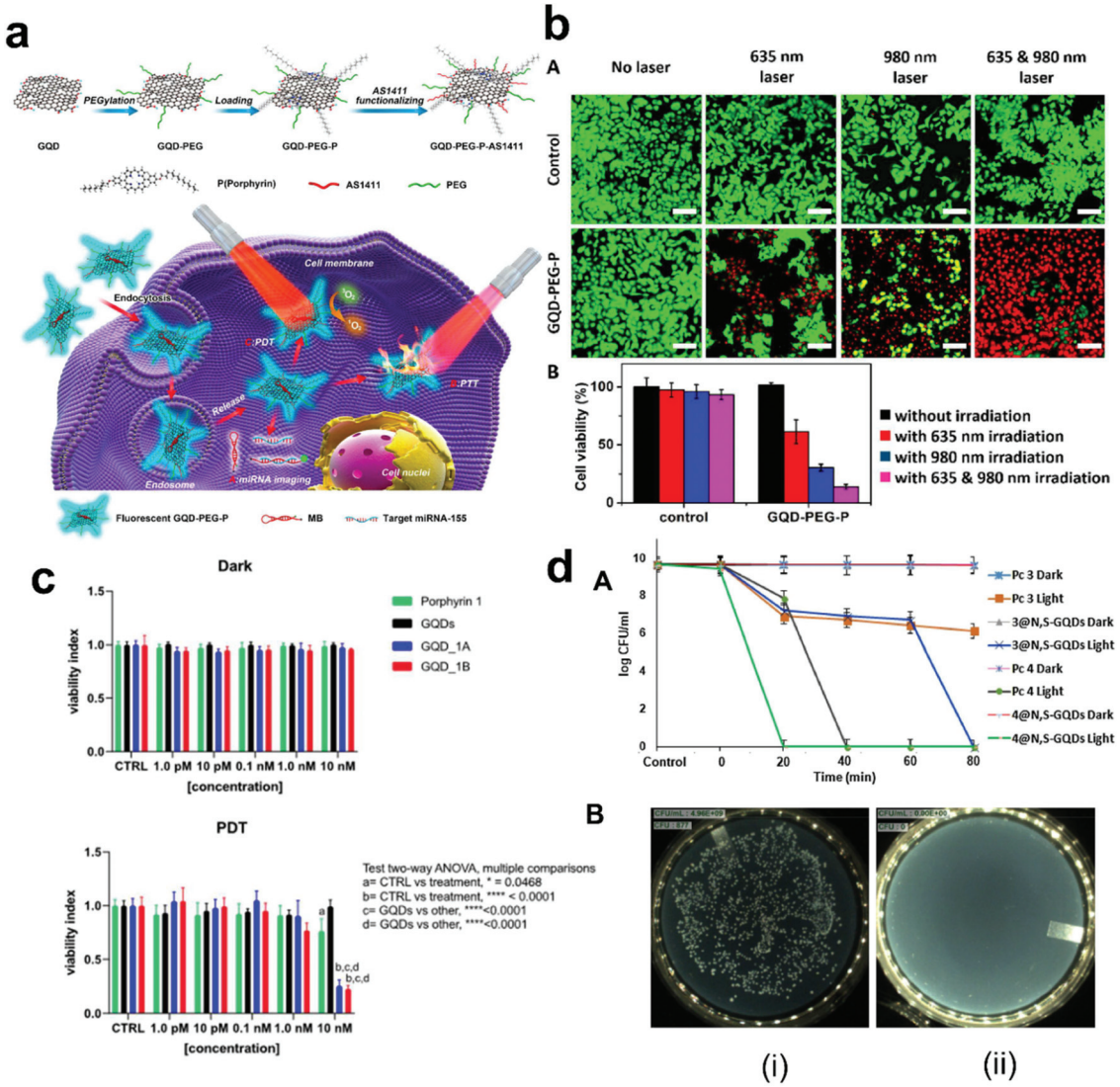

Fig. 9 Showing PDT and PTT effect of GQD-Pp/Pc conjugates (a) Schematic showing the theranostic application of GQD-PEG-P for the detection of intracellular miRNA and combined PTT/PDT effect. (b(A)) Confocal imaging of A549 treated with GQD-PEG-P with laser irradiation and treated with calcein-AM (live: green) and PI (dead: red). Scale bar: 40 μm. (b(B)) Cell viability of A549 when treated with GQD-PEG-P in dark and upon laser irradiation. Reprinted with permission from ref. 276 Copyright 2016, ACS. (c) Viability of T-47D cells treated with porphyrin 1, GQDs, GQD_1A, and GQD_1B at different concentrations, nonirradiated ("Dark") and irradiated ("PDT") with white light. Reprinted with permission from ref. 18 Copyright 2021, ACS. (d(A)) Phototoxicity studies: *S. Aureus* in the presence of ZnPc (3), quaternized derivative ZnPc (4), 3@N,S-GQD and 4@N,S-GQD with light and in the dark. (d(B)) Agar plates depicting *S. Aureus* colonies after treatment with 5% DMSO in PBS as the control (B(i)) and 3@N,S-GQD (B(ii)) after 80 min irradiation. Reprinted with permission from ref. 287 Copyright 2021, Elsevier B.V.

tration of 120 μg mL^{-1} but showed a PDT effect upon photoexcitation.[196] Nwahara *et al.* constructed a hybrid system, BODIPY@GQD/ZnPc, consisting of three PDT agents to increase the PDT effect. The hybrid system gave a higher ϕ_Δ due to the increase in triplet state population compared to the individual ZnPc and GQD/ZnPc moieties.[290]

4.4.2 Photodynamic antimicrobial chemotherapy. There is a pressing need to broaden the horizons of antibiotic research and development.[4,291–293] Interestingly, various micro-organisms and parasites can be inactivated by light, and based on this phenomenon, Pc can exhibit high photochemical activity and act as a potential photosensitizer (due to its high triplet quantum yield).[293] Feng *et al.* reported that with the introduction of porphyrin in carbon (CDs) they exhibited high antibacterial action by producing singlet oxygen under red light irradiation. Laser Scanning Confocal Microscopy (LSCM) imaging showed that the carbon dots (CDs) stick to the bacteria and generate ROS when exposed to red light to kill them. *In vitro* pigskin tests also revealed the antibacterial efficacy of CDs when exposed to a 638 nm laser.[294] This family of compounds had better photostability and absorption in the red area, allowing deeper ROS species production in tissues for longer.[108,168,301] Recently, Mei *et al.* demonstrated the antimicrobial properties of chitosan oligosaccharide-functiona-

lized GQDs (GQDs-COS) based on the synergistic combination of PDT, PTT, and chemotherapy against Gram-positive and Gram-negative bacteria.[160] The results indicated that photodynamic antimicrobial chemotherapy (PACT) can be a potential strategy to develop novel antibiotics to combat antimicrobial resistance. Using similar principles, GQD-Pp/Pc hybrid systems can be explored to develop a new era of PACT *via* ROS generation. ROS causes random oxidation of DNA, RNA, and/or lipid, leading to bacterial destruction, and thus preventing the development of specific resistance mechanisms in bacteria.[295,297]

Sen *et al.* recently reported the antibacterial activity of novel ZnPcs (3,4)-containing octa-imines and their nanoconjugates (3@N,S-GQDs and 4@N,S-GQDs) in *S. aureus*. As the singlet oxygen production increased for **3**@N,S-GQDs and **4**@N,S-GQDs compared to ZnPcs (**3**,**4**) alone, photoactivity resulted in complete cell destruction. Fig. 9d (A) and (B) and Table 4 show the existence of the bacteria colonies before and after treatment, respectively. This implies that the nanoconjugate has better activity than that of the unconjugated Pc alone. The enhanced activities of **3**@N,S-GQDs and **4**@N,S-GQDs compared to Pcs alone (**3**,**4**) could be due to the high ability of GQDs to bind to the cellular membranes. GQDs may disrupt the membrane and cause a canal large enough to allow PS to enter the cytoplasm. After entering the cell, they may prevent protein synthesis and DNA replication in addition to generating singlet oxygen.[287] Openda *et al.* reported that in comparison to other Pcs and conjugates, indium phthalocyanines (InPc) conjugated with GQDs demonstrated greater photo-antibacterial action. In comparison to only Pc, conjugate InPc@GQDs and ZnPc@GQDs were found to be highly effective, causing a 9.68 and 3.77 log reduction of bacteria at 10 μM, respectively[288] (Table 4).

4.4.3 Bioimaging. Monodisperse nanoparticles made of biocompatible building block conjugates can be useful in developing multipurpose new optical imaging systems and enhancing the therapeutic index.[6,298] In the case of near-infrared fluorescence imaging (NIRFI), magnetic resonance imaging (MRI), positron emission tomography (PET), and dual modal PET-MRI, nanoporphyrins can be employed as amplifiable multimodality nanoprobes. Nanoporphyrins considerably improve the imaging sensitivity for tumour identification by suppressing the background in the blood and preferentially accumulating and amplifying signals in tumours.[69] Biocompatible porphysomes can also be functionalized with receptor ligands to target nanoparticles or chelated with paramagnetic metal ions to serve as contrast agents in PET, MRI, and *in vivo* fluorescence imaging.[298] In the case of PDT, bioimaging of compounds is important for deciding the PDT dosimetry. Bioimaging helps to decide various matrices, such as the amount of PS at the site of treatment before and after PDT. However, metalloporphyrin/MPc-nanoparticle conjugates suffer from low fluorescence, which becomes a limitation in imaging. Thus, to overcome the reduced fluorescence of Pc, Nwahara *et al.* synthesized an assembly of gold nanoparticles (AuNPs) on functional GQD-Pcs conjugates, where imaging could be done through Raman spectroscopy of GQDs. The surface-enhanced Raman scattering of GQDs increased by 32-fold due to the chemisorbed AuNPs. Another important feature for PDT of this hybrid is that it had an increased singlet oxygen quantum yield. The composite system showed a high triple quantum yield due to the heavy atom effect of Au, which translated to a high singlet quantum yield as high as 87%. These remarkable features make the composite system a unique Raman-based PDT dosimetric agent.[299]

Table 4 Comparison of the phototherapeutic effect of porphyrin (Pp), GQDs, and the GQD-Pp hybrid system

Sl. no.		Singlet quantum yield (ϕ_Δ)	Cell viability (Conc.)	Wavelength of laser and duration of irradiation	Cytotoxicity studied in cancer/bacterial cells	Ref.
1	GQD-PEG-P	1.08	14% (100 μg mL^{-1}) 61.3% (100 μg mL^{-1}) 30.5% (100 μg mL^{-1})	635 nm and 980 nm for 10 min 635 nm for 10 min 980 nm for 10 min	A549 lung cancer cells	276
2	NGQDs	—	50% (14.2 μg mL^{-1})	625 nm for 30 min	MCF-7 breast cancer cells	192
	B-NGQDs	—	50% (14.4) μg mL^{-1})			
	SnPp	0.59	50% (11.2 μg mL^{-1})			
	SnPp-B-NGQDs	0.79	50% (10.4 μg mL^{-1})			
3	Porphyrin 1	0.47	50% (10–100 nM)	White light for 90 s	T-47D breast cancer cells	18
	GQD	0.07	—			
	GQD_1A	0.51	25% (10 nM)			
	GQD_1B	0.25	25% (10 nM)			
4.	ZnPc (3)	0.23	0.09% (10 μM)	680 nm for 80 min	*S. aureus* (Gram positive bacteria)	288
	quaternized derivative ZnPc (4)	0.31	0% (0.5 μM)	680 nm for 40 min		
	3@N,S-GQD	0.32	0% (10 μM)	680 nm for 80 min		
	4@N,S-GQD	0.42	0% (0.5 μM)	680 nm for 20 min		
5	Pc	0.22	24% (10 μM)	670 nm for 120 min	*S. aureus* (Gram positive bacteria)	287
	ZnPc	0.72	0.23% (10 μM)			
	InPc	0.75	0.14% (10 μM)			
	Pc@GQD	0.2	75% (10 μM)			
	ZnPc @GQD	0.77	0.12% (10 μM)			
	InPc@GQD	0.79	0% (10 μM)			

Santos *et al.* studied the cellular distribution of GQDs, GQD-Pp nanohybrids (GQD_1A and GQD_1B) and Pp in T-47D cells (Fig. 10a). Confocal imaging of porphyrin showed red fluorescence, which appeared as large bright aggregates preferentially at the periphery of the plasma membrane and as single spots in the cytoplasm. GQDs without porphyrin appeared green with some bright spots due to vesicular accumulation. GQD-Pp showed a red staining pattern, which encompassed manly bright spots in the cytoplasm, similar to porphyrin **1**. The fluorescence of the GQD-Pp nanohybrid inside the cells was visible at low concentration of 10 nM similar to that of porphyrin **1** at a higher concentration of 1 mM. This indicates the better internalization of the GQD-Pp hybrid system than porphyrin alone.[18] Cao *et al.* showed that GQD-PEG-P could discriminate cancer cells (A549) from somatic cells (HDF cells) due to the intrinsic fluorescence of GQD (Fig. 10b). The GQD-PEG-P-loaded molecular beacon (MB) facilitated gene delivery for the detection of cancer-associated microRNA (miRNA), as visible from the green color in A549 cells.[276]

Menilli *et al.* used LysoTracker Green DND-26, an acidic organelle marker, to visualise the intrinsic fluorescence of GO-Pp and GQD-Pp hybrids to determine the intracellular distribution of these Pp complexes in T24 human bladder cancer cells (porphyrin channel). TMPyP and ZnTMPyP in the free form were mainly carried to the lysosomes, as evidenced by the high co-localization (yellow) of the porphyrin red fluorescence with the green fluorescence of LysoTracker. The GO and GQD hybrids showed similar behaviour. It is worth noting that substantial aggregates of GO hybrids could be seen outside the cells, indicating that it was difficult for these hybrids to be fully internalised. This study suggests that the GO-complex required a very high concentration to have any photosensitizing effect[119] (Fig. 10c and d).

4.4.4 Drug delivery. Nanovehicles are used to deliver photosensitizers for photodynamic treatment (PDT) because of their enhanced penetration and retention effect; however, there are still drawbacks such as premature leakage and non-selective release of the photosensitizer.[300] Nanoporphyrins can also be used as programmable nanocarriers for the delivery of medications or therapeutic radio-metals into tumours. Nanoparticle-based medication delivery systems encounter blood as the initial biological barrier. Interactions with blood proteins and lipoproteins can induce the dissociation of nanoparticles, resulting in premature drug release. To improve the structural stability of GQDs in the blood circulation, GQDs based on porphyrin conjugates may be helpful.[69] Porphyrins and related compounds, particularly their derivatives, accumulate in cancerous tissues such as sarcomas and mammary carcinomas, and thus can be employed as drug transporters. Except for haematological malignancies, the accumulation of these substances in lymph nodes may reduce their therapeutic efficacy against practically all cancers.[298]

A novel multicomponent coordination self-assembly strategy based on the combination of histidine-containing short peptides, photosensitizers (Pp), and metal ions to design and engineer metallo-nanodrugs for antitumor therapy is based on the cooperative coordination of histidine residues and porphyrin derivatives (Fig. 11a). Zinc ion-coordinated multicomponent self-assembly with a photosensitizer yields spherical metallo-nanodrugs quickly (Fig. 11b and c). Surprisingly, metallo-nanodrugs exhibit both colloidal stability and burst release behaviour in the tumour microenvironment, complying with pH and glutathione (GSH) level variations. The robustness and flexibility of various coordination interactions with short peptides and photosensitizers underpin these behaviors. The constructed metallo-nanodrugs exhibited improved tumor accumulation, extended blood circulation, and tumor ablation[301] (Fig. 11d and e).

5. Current challenges, future perspectives, and conclusion

GQD-based porphyrin nanocomposites can allow specific targeting, extended tissue lifetime, drug delivery, immune tolerance, photophysical, electrochemical, and bioactive properties, healing and repair of damaged organs, biomimetic function, improved hydrophilicity, and cancer theranostics, depending on their kinetics, structure–function relationships, *etc*.[6,298] The tendency of nanohybrids to undergo intersystem crossing to an excited triplet state allows their use in therapeutic applications such as PDT and PTT. Surface modifications of Pp/Pc have helped to regulate their physicochemical, fluorescence, and pharmacological properties, which can permit their use for both diagnostic and therapeutic effects in fluorescence-guided tumor dissection and imaging. However, it is critical to study the pharmacokinetics and biodistribution of GQD-Pp/Pc conjugates before using them as nanoprobes for *in vivo* imaging. There are various challenges in designing GQD-porphyrin/Pc nanocomposites due to (i) the "uncertainty" of functionalization on the surface of GQDs will alter the conjugation of porphyrin or Pc, which will hamper the reproducibility, (ii) challenge of getting a high-quality single layer of GQDs with a narrow size distribution and high yield for their large-scale industrial and cost-effective production, and (iii) achieving nanocomposites with compositional and structural complexity, while preserving the monodispersity to create uniform and well-defined nanoparticles of various elemental compositions, sizes, and shapes as well as facet control *via* interface engineering. Fascinatingly, we envision meeting these challenges by integrating the special topographies of these single components into efficient and robust nanohybrid structures, which will result in novel and amplified features. Both Pp/Pc and GQDs present multiple options to govern their optical, magnetic, and electronic properties *via* easy and well-established synthetic methods. The multifunctional hybrid systems of GQD-Pp/Pc have been developed as promising novel materials for sensing, organic electronics, catalysis, various types of light-harvesting systems, and therapeutic applications, whereas in the arena of ecological, bio-analysis, and energy-related areas more studies need to be conducted together with

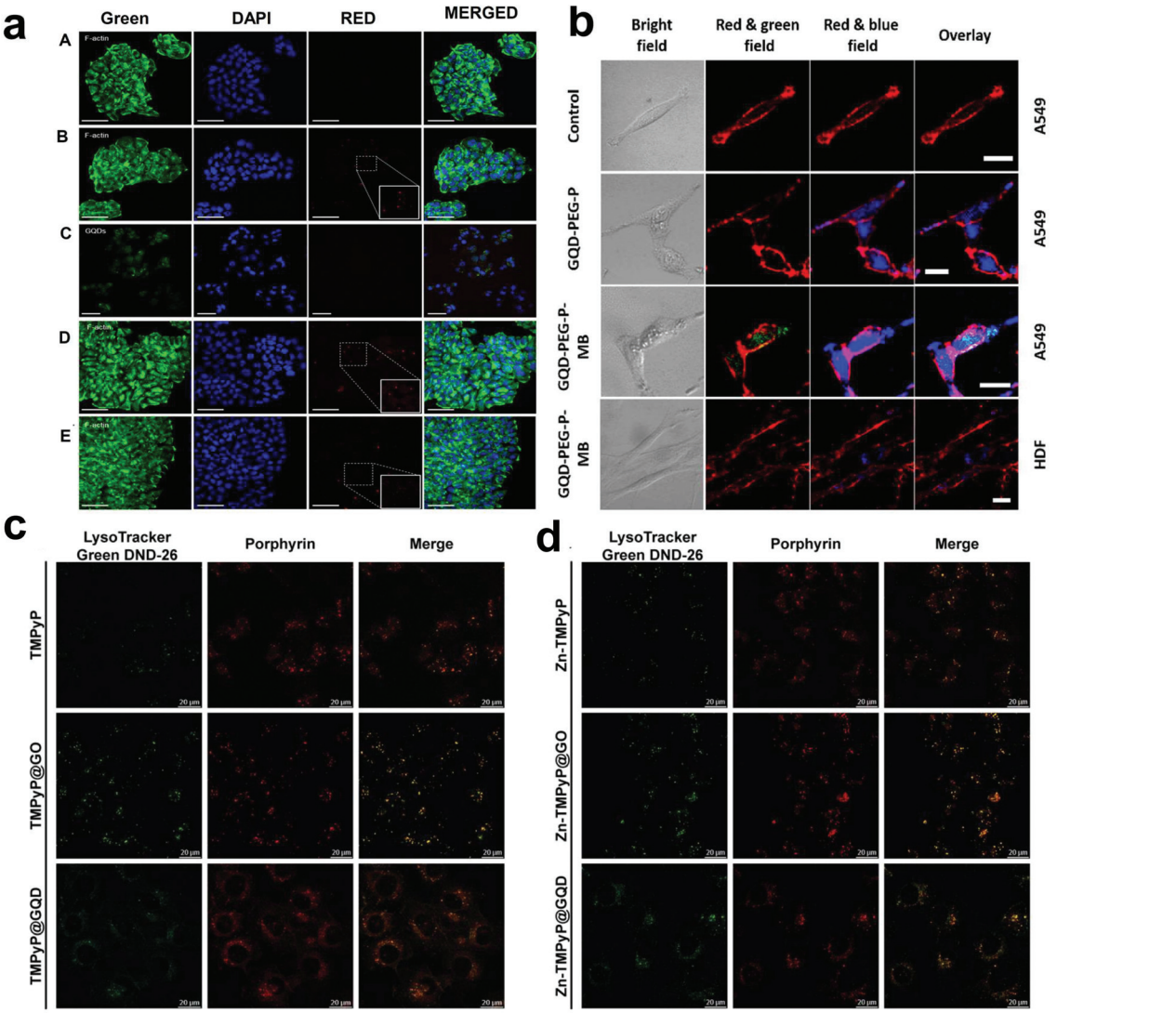

Fig. 10 (a) Confocal images of the cellular distribution of porphyrin, GQDs and GQD-Pp in T-47D cells. Cells were not exposed to any compound (control, A) or were exposed to porphyrin 1 (B), GQD (C), or the hybrids GQD-1A and GQD_1B (E). F-actin is labeled in green in panels A, B, D, and E and the nuclei marker (DAPI) is shown in blue. Scale bar is 20 mm. Reprinted with permission from ref. 18 Copyright 2021, ACS. (b) Confocal microscopy images of A549 cells transfected by GQD-PEG-P. Scale bar: 20 μm. Reprinted with permission from ref. 276 Copyright 2016, the American Chemical Society. Intracellular localization of TMPyP (c) and Zn-TMPyP (d) in the free form (top) and hybridized with GO (center) and GQDs (bottom).

chemical yield. GQDs-Pp/Pc hybrids as electrode materials may satisfy many needs of future power sources, such as high power densities and energy, improved cyclic stability in electrodes, electrical conductivity, long lifetime, safety, and environmental benignity. This facet of the challenges provides more prospects for scientists working in the field of materials-based research, and it is strongly believed that GQDs can meet the higher expectations in future applications. The investigation of the physical and medical properties of GQDs is still in progress with natural substitutes. Maybe this will be an eye-opening material for drug or gene delivery and beyond. As suitable, dictating their arrangement in specific environments, this hybrid system can show improved medicinal and site-localizing properties. To achieve this goal, new design concepts for functional GQD-Pp/Pc are strongly necessary. This study inspires us to elucidate opportunities associated with newer analogues of Pp and their derivatives as full-fledged therapeutic agents as the basis for preparing drug conjugates, which is required to further to employ their appropriate status in contemporary medicine. The result is considered a sign of even more impressive microbial eradication efforts that are still to come. From a conceptual viewpoint, Pp/Pc can be observed as essential for the development of GQD-Pp/Pc (GPP) conjugates.

In this contribution, we focused on the recent examples reported in the literature illustrating the integration of carbon nanomaterials (*i.e.*, graphene quantum dots) and Pp/Pc in disclosing structure–property trends to guide experimentalists towards a more rational design of nanohybrid systems. These

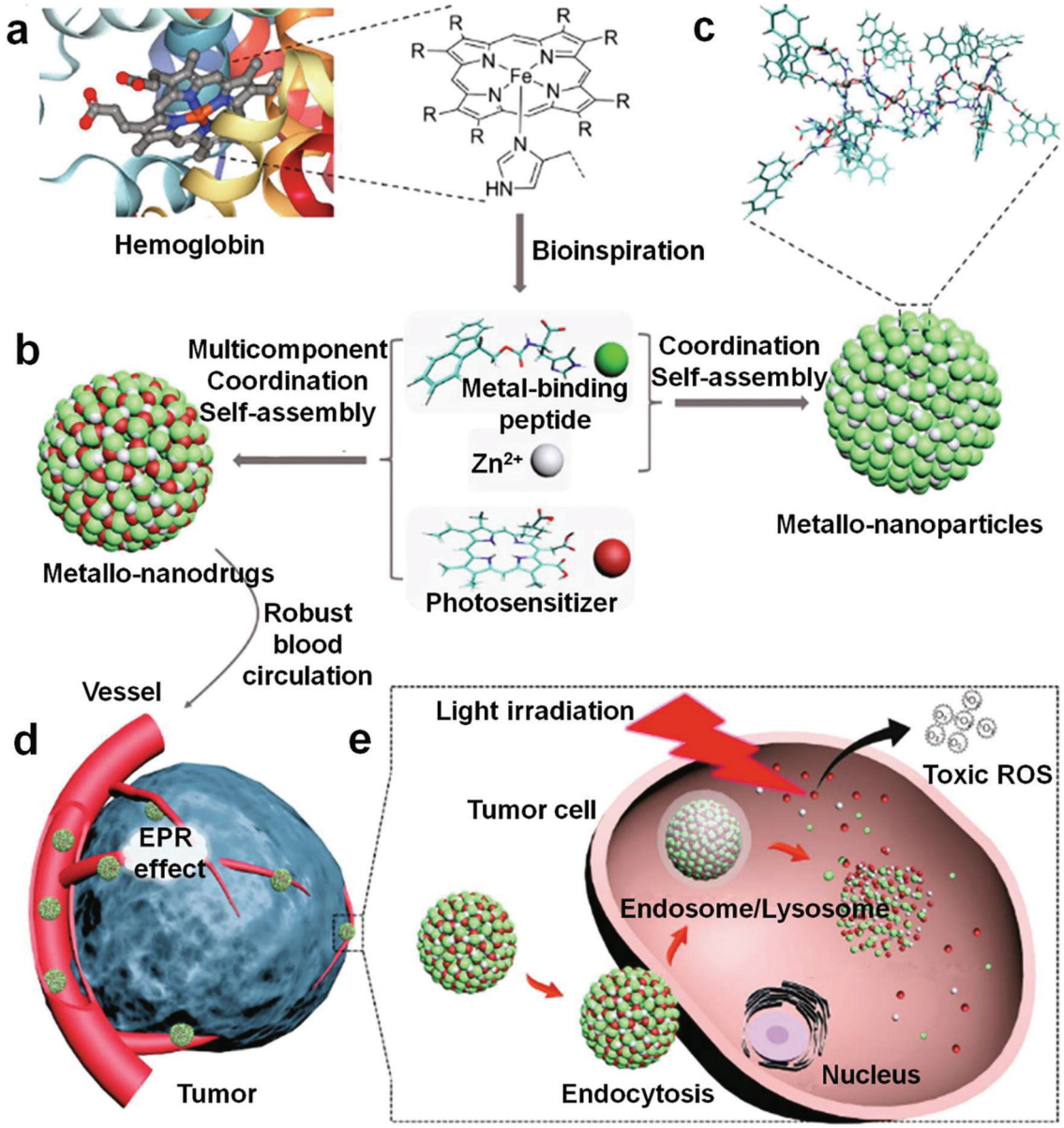

Fig. 11 Schematic diagram of (a) metalloporphyrin coordination for effective anticancer PDT. (b) Metalloporphyrin nanodrugs are formed by the cooperative coordination of short peptides and photosensitizers in the presence of zinc ions. (c) Pattern of metal-binding peptide and Zn^{2+} molecular organisation. (d) The EPR effect causes an accumulation of cancers. (e) Cellular internalisation of metalloporphyrin nanoparticles and efficient PDT.[153] Copyright 2018, ACS.

hybrids have become a treasure trove in which promising photochemical energy harvesting and therapeutic applications are emerging with novel examples of molecular organization. In summary, the field of biohybrid materials has been merging in the last few decades with that of PS, enabling the implementation of several biomedical technologies with enormous future impact. Accordingly, photosensitizing biohybrid materials represent a new generation of PS systems with improved features regarding their behavior in biological media. Importantly, the wide variety of biomolecular structures available in nature makes this approach versatile, allowing tuning of the type of biohybrid depending on the intended application or the target tissue. Supramolecular chemistry of these novel systems using weak to fairly strong binding motifs is emerging and should furnish future avenues for integration into nanoscience and nanotechnology developments. Thus, the intrinsic physicochemical properties of GQD-Pp/Pc will depend on the accuracy of controlling their shape and size. Because of the inherent synthetic control available for the design of GQD-based materials, the optical sensing approach has potential to be highly versatile for various target analytes. Consequently, the large range of possible bond orders of GQD-Pp/Pc hybrid systems offers fertile ground for chemical modification. The preparation of hybrids with high bond

orders is usually challenging because their moieties are highly reactive. Undoubtedly, this reactivity can be used in catalytic activities. GQD-Pp/Pc hybrid systems exhibit multiple bonding features at one extreme, while favoring definite conformations, resulting in various physical properties such as photoluminescence and magnetism. Increasing evidence implies that the conjugation of GQD-Pp/Pc hybrid systems can be employed in catalytic processes, which has proven to be popular because these preorganized structures have many tunable features, such as bond order, polarity, and complementarity, facilitating multisite activation-reactivity unattainable with truly monomolecular species. These nanohybrids can also be advantageous in dye-sensitised solar cells, photodynamic therapy, and photocatalysis as analogous uniformly arranged similar structures operate as photosensitizers and electron transmission medium.[184] If the intrinsic properties of porphyrin macrocycles, that is, the incorporation of metal centers capable of axial ligation of adducts, are preserved upon coupling with graphene, further options for the functionalization of graphene nanostructures will emerge. This immense interest stems from their ability to serve as ligands for a variety of metals to catalyze many reactions and absorb and convert light into other forms of energy. Also, we addressed the exemplary developments regarding the fabrication, control, and functionality of hybrid and bio-inspired nanosystems and architectures. As fully synthetic, and often privileged, macrocycles, Pp analogs have a rich future in the design of drug conjugates.

This review addressed the efforts to improve the delivery and uptake of porphyrinoid-based compounds in a myriad of applications. The premiere biomedical application of porphyrinoids is as photosensitizers in PDT. Their synthetic versatility, long-range order, and rich host–guest chemistry make these nanohybrids an ideal platform for identifying design features for advanced functional materials. We anticipate that with this review, new archetypes and strategies in the application of Pp and its derivatives will progressively flourish and lead to unprecedented chemical and structural tunability. To enhance their stabilization, porphyrin-containing polymers have been developed. To develop new PSs, various properties such as biocompatibility, biodegradability, and tumor selectivity must also be considered.

The highly polar nature of these compounds is also problematic in separating the products from the unwanted by-products. In this regard, the late-stage introduction of GQD moieties with Pp/Pc is desirable, and click chemistry is ideal for this purpose. Consequently, high reactivity is required for surface modification reactions. Because of its high efficiency, click chemistry enables efficient surface modification. Using the CuAAC reaction, various surfaces can be efficiently functionalized with porphyrin units.

Consequently, porphyrin chemists can now focus on exploring the properties and functions of sophisticated porphyrins without much synthetic effort. The important goal for chemists is to achieve intriguing and useful properties and functions of materials, not just their synthesis. Continued work in these emerging fields is of great value to understand their functions. The emergence of hybrid-Pp/Pc opens up new opportunities in different branches of science and technology primarily because of their conducive biocompatibility, tunable bandgaps, and unique optoelectronic properties, namely, photoluminescence and fluorescence.

Author contributions

Sujata Sangam has finalized the entire manuscript. Puja Prasad has contributed in writing, making figures, and tables along with Sujata Sangam. Simran Jindal collated papers related to the application in catalysis and biosensing. Aakanksha Agarwal has collated the papers related to energy conversion and future prospects. Basu Dev Banerjee has worked on the references. Monalisa Mukherjee has conceptualized, supervised, and proposed the title.

Conflicts of interest

There are no conflicts to declare.

Acknowledgements

Sujata Sangam is grateful to Council of Scientific & Industrial Research (CSIR)–University Grants Commission (UGC) for providing financial support and AICCRS/AIB, Noida. Puja Prasad thanks IITD and CSIR for SRA position (pool no. 9031-892A). Monalisa Mukherjee thanks the Department of Science and Technology (DST) and Science and Engineering Research Board (SERB) (EMR/2016/00561) for funding and Amity University Uttar Pradesh (AUUP, Noida) for providing research infrastructure and library facility.

References

1 G. Xue, S. Yu, Z. Qiang, L. Xiuying, T. Lijun and L. Jiangrong, *Anal. Chim. Acta*, 2020, **1108**, 46–53.
2 R. Paolesse, S. Nardis, D. Monti, M. Stefanelli and C. di Natale, *Chem. Rev.*, 2017, **117**, 2517–2583.
3 D. K. Deda, B. A. Iglesias, E. Alves, K. Araki and C. R. S. Garcia, *Molecules*, 2020, **25**, 2080.
4 L. Jiang, C. R. R. Gan, J. Gao and X. J. Loh, *Small*, 2016, **12**, 3609–3644.
5 M. Imran, M. Ramzan, A. K. Qureshi, M. A. Khan and M. Tariq, *Biosensors*, 2018, **8**, 1–17.
6 N. Rabiee, M. T. Yaraki, S. M. Garakani, S. M. Garakani, S. Ahmadi, A. Lajevardi, M. Bagherzadeh, M. Rabiee, L. Tayebi, M. Tahriri and M. R. Hamblin, *Biomaterials*, 2020, **232**, 119707.
7 H. Wu, X. Li, M. Chen, C. Wang, T. Wei, H. Zhang and S. Fan, *Electrochim. Acta*, 2018, **259**, 355–364.

8 H. Montaseri, C. A. Kruger and H. Abrahamse, *Int. J. Mol. Sci.*, 2020, **21**, 3358.
9 J. Wang, Y. Zhong, X. Wang, W. Yang, F. Bai, B. Zhang, L. Alarid, K. Bian and H. Fan, *Nano Lett.*, 2017, **17**, 6916–6921.
10 G. Magna, F. Mandoj, M. Stefanelli, G. Pomarico, D. Monti, C. Di Natale, R. Paolesse and S. Nardis, *Nanomaterials*, 2021, **11**, 1–21.
11 D. Mondal and S. Bera, *Adv. Nat. Sci.: Nanosci. Nanotechnol.*, 2014, **5**, 033002.
12 J. M. Gottfried, *Surf. Sci. Rep.*, 2015, **70**, 259–379.
13 A. Aggarwal, D. Samaroo, I. R. Jovanovic, S. Singh, M. P. Tuz and M. R. Mackiewicz, *J. Porphyrins Phthalocyanines*, 2019, **23**, 729–765.
14 A. B. Sorokin, *Chem. Rev.*, 2013, **113**, 8152–8191.
15 W. Auwärter, D. Écija, F. Klappenberger and J. V. Barth, *Nat. Chem.*, 2015, **7**, 105–120.
16 X. Zhang, M. C. Wasson, M. Shayan, E. K. Berdichevsky, J. Ricardo-Noordberg, Z. Singh, E. K. Papazyan, A. J. Castro, P. Marino, Z. Ajoyan, Z. Chen, T. Islamoglu, A. J. Howarth, Y. Liu, M. B. Majewski, M. J. Katz, J. E. Mondloch and O. K. Farha, *Coord. Chem. Rev.*, 2021, **429**, 213615.
17 Z. Zhong, J. Liu, X. Xu, A. Cao, Z. Tao, W. You and L. Kang, *J. Mater. Chem. A*, 2021, **9**, 2404–2413.
18 C. I. M. Santos, L. Rodríguez-Pérez, G. Gonçalves, C. J. Dias, F. Monteiro, M. do A. F. Faustino, S. I. Vieira, L. A. Helguero, M. Á. Herranz, N. Martín, M. G. P. M. S. Neves, J. M. G. Martinho and E. M. S. Maçôas, *ACS Appl. Nano Mater.*, 2021, **4**, 13079–13089.
19 L. B. Kong, W. Que, K. Zhou, S. Li and T. Zhang, in *Advanced Structured Materials*, Springer Verlag, 2017, vol. 83, pp. 177–243.
20 M. Zhang, B. Yuan, S. Z. Kang, L. Qin, G. Li and X. Li, *RSC Adv.*, 2015, **5**, 42063–42068.
21 A. Wang, J. Ye, M. G. Humphrey and C. Zhang, *Adv. Mater.*, 2018, **30**, 1705704.
22 D. Mondal, S. Bera, L. C. Nene, M. E. Managa, D. O. Oluwole, D. M. Mafukidze, Y. R. Kumar, K. Deshmukh, S. K. K. Pasha, Z. Bing, Z. Qiang, T. Yiwei, L. Xiuying, L. Jianrong, D. M. Mafukidze, T. Nyokong, O. J. Achadu, I. Uddin and T. Nyokong, *J. Mol. Struct.*, 2016, **317**, 12–25.
23 Y. Liu, S. Li, K. Li, Y. Zheng, M. Zhang, C. Cai, C. Yu, Y. Zhou and D. Yan, *Chem. Commun.*, 2016, **52**, 9394–9397.
24 C. I. M. Santos, G. Gonçalves, M. Cicuéndez, I. Mariz, V. S. Silva, H. Oliveira, F. Campos, S. I. Vieira, P. A. A. P. Marques, E. M. S. Maçôas, M. G. P. M. S. Neves and J. M. G. Martinho, *Carbon*, 2018, **135**, 202–214.
25 J. L. Delgado, M. A. Herranz and N. Martin, *J. Mater. Chem.*, 2008, **18**, 1417–1426.
26 J. Liu, R. Li and B. Yang, *ACS Cent. Sci.*, 2020, **6**, 2179–2195.
27 B. I. Kharisov, O. V. Kharissova, A. V. Dimas, I. G. D. L. Fuente and P. Y. Mendez, *J. Coord. Chem.*, 2016, **69**, 1125–1151.
28 M. J. Allen, V. C. Tung and R. B. Kaner, *Chem. Rev.*, 2010, **110**, 132–145.
29 P. Tian, L. Tang, K. S. Teng and S. P. Lau, *Mater. Today Chem.*, 2018, **10**, 221–258.
30 W. Chen, G. Lv, W. Hu, D. Li, S. Chen and Z. Dai, *Nanotechnol. Rev.*, 2018, **7**, 157–185.
31 H. Sun, N. Gao, K. Dong, J. Ren and X. Qu, *ACS Nano*, 2014, **8**, 6202–6210.
32 L. Lin, M. Rong, F. Luo, D. Chen, Y. Wang and X. Chen, *Trends Analyt. Chem.*, 2014, **54**, 83–102.
33 M. H. M. Facure, R. Schneider, J. B. S. Lima, L. A. Mercante and D. S. Correa, *Electrochem*, 2021, **2**, 490–519.
34 M. C. Biswas, M. T. Islam, P. K. Nandy and M. M. Hossain, *ACS Mater. Lett.*, 2021, **3**, 889–911.
35 A. C. Power, B. Gorey, S. Chandra and J. Chapman, *Nanotechnol. Rev.*, 2018, **7**, 19–41.
36 D. Ghosh, K. Sarkar, P. Devi, K. H. Kim and P. Kumar, *Renewable Sustainable Energy Rev.*, 2021, **135**, 110391.
37 S. Kadian, S. K. Sethi and G. Manik, *Mater. Chem. Front.*, 2021, **5**, 627–658.
38 X. Li, M. Rui, J. Song, Z. Shen and H. Zeng, *Adv. Funct. Mater.*, 2015, **25**, 4929–4947.
39 T. Sun, Y. Zhang, R. Yan, Y. Jiang and Y. Zhao, *Part. Part. Syst. Charact.*, 2021, **38**, 2000261.
40 N. Rabiee, M. Bagherzadeh, A. M. Ghadiri, Y. Fatahi, N. Baheiraei, M. Safarkhani, A. Aldhaher and R. Dinarvand, *Sci. Rep.*, 2021, **11**, 1–15.
41 L. M. Mateo, Q. Sun, S. X. Liu, J. J. Bergkamp, K. Eimre, C. A. Pignedoli, P. Ruffieux, S. Decurtins, G. Bottari, R. Fasel and T. Torres, *Angew. Chem., Int. Ed.*, 2020, **59**, 1334–1339.
42 B. Mandal, S. Sarkar and P. Sarkar, *J. Phys. Chem. C*, 2015, **119**, 3400–3407.
43 A. R. Monteiro, M. G. P. M. S. Neves and T. Trindade, *ChemPlusChem*, 2020, **85**, 1857–1880.
44 K. Ariga, V. Malgras, Q. Ji, M. B. Zakaria and Y. Yamauchi, *Coord. Chem. Rev.*, 2016, **320–321**, 139–152.
45 E. Prigorchenko, L. Ustrnul, V. Borovkov and R. Aav, *Porphyrin Science By Women (In 3 Volumes)*, 2020, pp. 816–833.
46 V. Almeida-Marrero, E. Van De Winckel, E. Anaya-Plaza, T. Torres and A. De La Escosura, *Chem. Soc. Rev.*, 2018, **47**, 7369–7400.
47 C. Zhang, W. Chen, T. Zhang, X. Jiang and Y. Hu, *J. Mater. Chem. B*, 2020, **8**, 4726–4737.
48 Z. Yang, L. Fan, X. Fan, M. Hou, Z. Cao, Y. Ding and W. Zhang, *Anal. Chem.*, 2020, **92**, 6727–6733.
49 E. Hwang, H. M. Hwang, Y. Shin, Y. Yoon, H. Lee, J. Yang, S. Bak and H. Lee, *Sci. Rep.*, 2016, **6**, 1–10.
50 J. N. Tiwari, V. Vij, K. C. Kemp and K. S. Kim, *ACS Nano*, 2016, **10**, 46–80.
51 J. F. Arambula and J. L. Sessler, *Chem*, 2020, **6**, 1634–1651.
52 M. D. Shirsat, T. Sarkar, J. Kakoullis, N. V. Myung, B. Konnanath, A. Spanias and A. Mulchandani, *J. Phys. Chem. C*, 2012, **116**, 3845–3850.

53 K. Nekoueian, M. Amiri, M. Sillanpää, F. Marken, R. Boukherroub and S. Szunerits, *Chem. Soc. Rev.*, 2019, **48**, 4281–4316.
54 K. Lagos, H. Buzzá, V. Bagnato and M. Romero, *Int. J. Mol. Sci.*, 2022, **23**, 22.
55 Y. Li, X. Zheng, X. Zhang, S. Liu, Q. Pei, M. Zheng and Z. Xie, *Adv. Healthcare Mater.*, 2017, **6**, 1–6.
56 N. Karousis, A. S. D. Sandanakaya, T. Hasobe, S. P. Economopoulos, E. Sarantopoulou and J. Tagmatarchis, *J. Mater. Chem.*, 2011, **21**, 109–117.
57 L. J. Chen, S. Chen, Y. Qin, L. Xu, G. Q. Yin, J. L. Zhu, F. F. Zhu, W. Zheng, X. Li and H. B. Yang, *J. Am. Chem. Soc.*, 2018, **140**, 5049–5052.
58 F. Lv, X. He, L. Lu, L. Wu and T. Liu, *J. Porphyrins Phthalocyanines*, 2012, **16**, 77–84.
59 D. Mondal and S. Bera, *Adv. Nat. Sci.: Nanosci. Nanotechnol.*, 2014, **5**, 033002.
60 D. Samaroo, E. Perez, A. Aggarwal, A. Wills and N. O'Connor, *Ther. Delivery*, 2014, **5**, 859–872.
61 L. M. Mateo, Q. Sun, S. Liu, J. J. Bergkamp, K. Eimre, C. A. Pignedoli, P. Ruffieux, S. Decurtins, G. Bottari, R. Fasel and T. Torres, *Angew. Chem.*, 2020, **132**, 1350–1355.
62 X. Fen, B. D. Phebus, L. Li and S. Chen, *Sci. Adv. Mater.*, 2015, **7**, 1990–2010.
63 G. Singh, H. Kaur, A. Sharma, J. Singh, H. K. Alajangi, S. Kumar, N. Singla, I. P. Kaur and R. P. Barnwal, *Front. Chem.*, 2021, **9**, 1–12.
64 A. Wang and W. Zhao, in *Chemical Reactions in Inorganic Chemistry*, UK, InTechOpen, 2018, pp. 9–29.
65 J. Xie, Y. Wang, W. Choi, P. Jangili, Y. Ge, Y. Xu, J. Kang, L. Liu, B. Zhang, Z. Xie, J. He, N. Xie, G. Nie, H. Zhang and J. S. Kim, *Chem. Soc. Rev.*, 2021, **50**, 9152–9201.
66 J. Ge, M. Lan, B. Zhou, W. Liu, L. Guo, H. Wang, Q. Jia, G. Niu, X. Huang, H. Zhou, X. Meng, P. Wang, C. S. Lee, W. Zhang and X. Han, *Nat. Commun.*, 2014, **5**, 1–8.
67 G. Botari, O. Trukhina, M. Ince and T Torres, *Coord. Chem. Rev.*, 2012, **256**, 2453–2477.
68 S. Supriya, V. S. Shetti and G. Hegde, *New J. Chem.*, 2018, **42**, 12328–12348.
69 L. Wei, H. Chen, R. Liu, S. Wang, T. Liu, Z. Hu, W. Lan, Y. Hu, Y. She and H. Fu, *J. Sci. Food Agric.*, 2021, **101**, 6193–6201.
70 G. Cárdenas-Jirón, Y. Figueroa, N. Kumar and J. M. Seminario, *J. Phys. Chem. C*, 2016, **120**, 2013–2026.
71 R. Bera, S. Mandal, B. Mondal, B. Jana, S. K. Nayak and A. Patra, *ACS Sustainable Chem. Eng.*, 2016, **4**, 1562–1568.
72 J. Du, N. Xu, J. Fan, W. Sun and X. Peng, *Small*, 2019, **15**, 1805087.
73 Z. Jin, P. Owour, S. Lei and L. Ge, *Curr. Opin. Colloid Interface Sci.*, 2015, **20**, 439–453.
74 A. Kole and D. S. Ang, *AIP Adv.*, 2018, **8**, 085009.
75 S. Wu, Q. He, C. Tan, Y. Wang and H. Zhang, *Small*, 2013, **9**, 1160–1172.
76 L. B. Drissi, H. Ouarrad, F. Z. Ramadan and W. Fritzsche, *RSC Adv.*, 2019, **10**, 801–811.
77 T. A. Tabish and S. Zhang, in *Comprehensive Nanoscience and Nanotechnology*, Elsevier, 2019, 1–5, 171–192.
78 B. Z. Ristic, M. M. Milenkovic, I. R. Dakic, B. M. Todorovic-markovic, M. S. Milosavljevic, M. D. Budimir, V. G. Paunovic, M. D. Dramicanin, Z. M. Markovic and V. S. Trajkovic, *Biomaterials*, 2014, **35**, 4428–4435.
79 M. Bacon, S. J. Bradley and T. Nann, *Part. Part. Syst. Charact.*, 2013, **31**, 415–428.
80 B. M. Min, S. Sakri, G. A. Saenz and A. B. Kaul, *ACS Appl. Mater. Interfaces*, 2021, **13**, 5379–5389.
81 X. Zhao, W. Gao, H. Zhang, X. Qiu and Y. Luo, *Graphene quantum dots in biomedical applications: Recent advances and future challenges*, Elsevier Inc., 2019, pp. 493–505.
82 P. N. Joshi, S. Kundu, S. K. Sanghi and D. Sarkar, in *Smart Drug Delivery Syst.*, ed. A. Sezer, IntechOpen, London, UK, 2016, pp. 159–197.
83 J. Shen, W. Chen, Z. Yang, G. Lv, J. Cao, D. Li and X. Liu, *Nano*, 2021, **16**, 2130001.
84 V. Bressi, A. Ferlazzo, D. Iannazzo and C. Espro, *Nanomaterials*, 2011, **11**, 1120.
85 S. Sangam, A. Gupta, A. Shakeel, R. Bhattacharya, A. K. Sharma, D. Suhag, S. Chakrabarti, S. K. Garg, S. Chattopadhyay, B. Basu, V. Kumar, S. K. Rajput, M. K. Dutta and M. Mukherjee, *Green Chem.*, 2018, **20**, 4245–4259.
86 V. K. Sagar, A. v. Veluthandath and P. B. Bisht, *J. Photochem. Photobiol., A*, 2020, **400**, 112614.
87 S. A. Prabhu, V. Kavithayeni, R. Suganthy and K. Geetha, *Carbon Lett.*, 2021, **31**, 1–12.
88 H. Chen, Z. Wang, S. Zong, P. Chen, D. Zhu, L. Wu and Y. Cui, *Nanoscale*, 2015, **7**, 15477–15486.
89 H. Zhao, R. Ding, X. Zhao, Y. Li, L. Qu, H. Pei, L. Yildirimer, Z. Wu and W. Zhang, *Drug Discovery Today*, 2017, **22**, 1302–1317.
90 G. M. Paternò, Goudappagouda, Q. Chen, G. Lanzani, F. Scotognella and A. Narita, *Adv. Opt. Mater.*, 2021, **9**, 2100508.
91 H. Lu, W. Li, H. Dong and M. Wei, *Small*, 2019, **15**, 1902136.
92 D. Iannazzo, A. Pistone, C. Celesti, C. Triolo, S. Patane, S. V. Giofre, R. Romeo, I. Ziccarelli,, R. Mancuso, B. Gabriele, G. Visalli, A. Facciola and A. D. Pietro, *Nanomaterials*, 2019, **9**, 282.
93 M. K. Kumawat, M. Thakur, R. B. Gurung and R. Srivastava, *Sci. Rep.*, 2017, **7**, 1–16.
94 Q. Li, S. Zhang and L. Dai, *J. Am. Chem. Soc.*, 2012, **134**, 18932–18935.
95 M. Mili, A. Jaiswal, V. Hada, S. S. Sagiri, K. Pal, R. Chowdhary, R. Malik, R. S. Gupta, M. K. Gupta, J. P. Chourasia, S. Hashmi, S. K. S. Rathore, A. K. Srivastava and S. Verma, *ChemistrySelect*, 2021, **6**, 9990–10001.
96 D. Iannazzo, A. Pistone, M. Salamo, S. Galvagno, R. Romeo, S. Giofre, C. Branca, G. Visalli and A. Pietro, *Int. J. Pharm.*, 2017, **518**, 185–192.

97 X. Li, S. P. Lau, L. Tang, R. Ji and P. Yang, *J. Mater. Chem. C*, 2013, **1**, 7308–7313.
98 S. Veeresh, H. Ganesh, Y. S. Nagaraju, M. Vandana, S. P. Ashokkumar, H. Vijeth, M. V. N. A. Prasad and H. Devendrappa, *Diamond Relat. Mater.*, 2021, **114**, 108289.
99 D. Qu, M. Zheng, J. Li, Z. Xie and Z. Sun, *Light: Sci. Appl.*, 2015, **4**, e364.
100 D. Qu, M. Zheng, L. Zhang, H. Zhao, Z. Xie, X. Jing, R. E. Haddad, H. Fan and Z. Sun, *Sci. Rep.*, 2014, **4**, 1–9.
101 B. Wagner, N. Dehnhardt, M. Schmid, B. P. Klein, L. Ruppenthal, P. Müller, M. Zugermeier, J. M. Gottfried, S. Lippert, M. U. Halbich, A. Rahimi-Iman and J. Heine, *J. Phys. Chem. C*, 2016, **120**, 28363–28373.
102 J. Campos, *Nat. Rev. Chem.*, 2020, **4**, 696–702.
103 K. H. Koh, S. H. Noh, T. H. Kim, W. J. Lee, S. C. Yi and T. H. Han, *RSC Adv.*, 2017, **7**, 26113–26119.
104 S. Dhar, T. Majumder, S. P. Mondal, M. R. Younis, G. He, J. Lin, P. Huang, P. Tian, L. Tang, K. S. Teng, S. P. Lau, M. J. Allen, V. C. Tung, R. B. Kaner, N. W. Street, M. Pereira, D. Lucas, M. J. F. Calvete, C. Lan, J. Zhao, L. Zhang, C. Wen, Y. Huang, S. Zhao, D. M. Tobaldi, D. Dvoranová, L. Lajaunie, N. Rozman, B. Figueiredo, M. P. Seabra, Y. Ding, W. Zhu, Y. Xie, X. Bu, S. Yang, Y. Bu, P. He, Y. Yang, G. Wang, T. Wu, X. Wang, A. Emrehan, J. Fan, Y. Min, Q. Xu, S. Sun, V. A. Online, J. Dong, L. Sun, H. Chen, Y. Wang, C. Wang, L. Dong, J. Hwan, S. Choi, Y. Jung, J. Sung, N. Sung, S. Cho, B. Walker, D. Soo, J. Shin, J. Hwa, A. B. Sorokin, D. Mondal, S. Bera, Y. Zhao, C. Hu, Y. Hu, H. Cheng, G. Shi and L. Qu, *Mater. Today Chem.*, 2018, **10**, 221–258.
105 T. van Tam, S. H. Hur, J. S. Chung and W. M. Choi, *Sens. Actuators, A*, 2015, **233**, 368–373.
106 J. Chen, W. Wu, F. Zhang, J. Zhang, H. Liu, J. Zheng, S. Guo and J. Zhang, *Nanoscale Adv.*, 2020, **2**, 4961–4967.
107 Y. R. Kumar, K. Deshmukh and S. K. K. Pasha, *RSC Adv.*, 2020, **10**, 23861–23898.
108 S. Sakthinathan, S. Kubendhiran, S. M. Chen, M. Govindasamy, F. M. A. Al-Hemaid, M. Ajmal Ali, P. Tamizhdurai and S. Sivasanker, *Appl. Organomet. Chem.*, 2017, **31**, 1–10.
109 C. Kong, G. Zhang, Y. Li, D. W. Lei and Y. T. Long, *RSC Adv.*, 2013, **3**, 3503–3507.
110 V. Georgakilas, M. Otyepka, A. B. Bourlinos, V. Chandra, N. Kim, K. C. Kemp, P. Hobza, R. Zboril and K. S. Kim, *Chem. Rev.*, 2012, **112**, 6156–6214.
111 D. Wu, Y. Liu, Y. Wang, L. Hu, H. Ma, G. Wang and Q. Wei, *Sci. Rep.*, 2016, **6**, 1–7.
112 J. Liu, J. Tang and J. J. Gooding, *J. Mater. Chem*, 2012, **22**, 12435–12452.
113 X. F. Zhang and X. Shao, *J. Photochem. Photobiol., A*, 2014, **278**, 69–74.
114 K. Ma, R. Wang, T. Jiao, J. Zhou, L. Zhang, J. Li, Z. Bai and Q. Peng, *Colloids Surf., A*, 2020, **584**, 124023.
115 R. Yamuna, S. Ramakrishnan, K. Dhara, R. Devi, N. K. Kothurkar, E. Kirubha and P. K. Palanisamy, *J. Nanopart. Res.*, 2013, **15**, 1399.
116 S. Tajik, Z. Dourandish, K. Zhang, H. Beitollahi, Q. Van Le, H. W. Jang and M. Shokouhimehr, *RSC Adv.*, 2020, **10**, 15406–15429.
117 S. Khoee and A. Sadeghi, *RSC Adv.*, 2019, **9**, 39780–39792.
118 P. Guo, P. Chen and M. Liu, *ACS Appl. Mater. Interfaces*, 2013, **5**, 5336–5345.
119 L. Menilli, A. R. Monteiro, S. Lazzarotto, F. M. P. Morais, A. T. P. C. Gomes, N. M. M. Moura, S. Fateixa, M. A. F. Faustino, M. G. P. M. S. Neves, T. Trindade and G. Miolo, *Pharmaceutics*, 2021, **13**, 1512.
120 M. A. Rajora, J. W. H. Lou and G. Zheng, *Chem. Soc. Rev.*, 2017, **46**, 6433–6469.
121 J. Touzeau, F. Barbault, F. Maurel and M. Seydou, *Chem. Phys. Lett.*, 2018, **713**, 172–179.
122 D. Larowska, A. Wojcik, M. Mazurkiewicz-Pawlicka, A. Malolepszy, L. Stobiński, B. Marciniak and A. Lewandowska-Andralojc, *ChemPhysChem*, 2019, **20**, 1054–1066.
123 F. Cheng, J. Zhu and A. Adronov, *Chem. Mater.*, 2011, **23**, 3188–3194.
124 X. Gao, B. Zhang, Q. Zhang, Y. Tang, X. Liu and J. Li, *Colloids Surf., B*, 2018, **172**, 207–212.
125 X. Xue, A. Lindstrom and Y. Li, *Bioconjugate Chem.*, 2019, **30**, 1585–1603.
126 A. T. P. C. Gomes, M. G. P. M. S. Neves and J. A. S. Cavaleiro, *An. Acad. Bras. Cienc.*, 2018, **90**, 993–1026.
127 B. de Zheng, J. Ye, Y. Y. Huang and M. T. Xiao, *Biomater. Sci.*, 2021, **9**, 7811–7825.
128 E. Park, D. Oh, S. Park, W. Kim and C. Kim, *APL Bioeng.*, 2021, **5**, 31510.
129 A. Hasani, J. N. Gavgani, R. M. Pashki, S. Baseghi, A. Salehi, D. Heo, S. Y. Kim and M. Mahyari, *Sci. Adv. Mater.*, 2017, **9**, 1616–1625.
130 A. Wang, J. Song, D. Jia, W. Yu, L. Long, Y. Song, M. P. Cifuentes, M. G. Humphrey, L. Zhang, J. Shao and C. Zhang, *Inorg. Chem. Front.*, 2016, **3**, 296–305.
131 S. M. Aly, M. R. Parida, E. Alarousu and O. F. Mohammed, *Chem. Commun.*, 2014, **50**, 10452–10455.
132 H. G. Jeong and M. S. Choi, *Isr. J. Chem.*, 2016, **56**, 110–118.
133 G. Xue, M. Zhiying, L. Xiuying, T. Lijun and L. Jianrong, *J. Fluoresc.*, 2020, **30**, 1463–1468.
134 N. Zheng, X. Li, S. Huangfu, K. Xia, R. Yue, H. Wu and W. Song, *Biomater. Sci.*, 2021, **9**, 4630–4638.
135 L. Zhang, D. Peng, R.-P. Liang and J.-D. Qiu, *Chem. – Eur. J.*, 2015, **21**, 9343–9348.
136 J. Bhaumik, A. K. Mittal, A. Banerjee, Y. Chisti and U. C. Banerjee, *Nano Res.*, 2015, **8**, 1373–1394.
137 Y. Zhou, X. Liang and Z. Dai, *Nanoscale*, 2016, **8**, 12394–12405.
138 M. Overchuk, M. Zheng, M. A. Rajora, D. M. Charron, J. Chen and G. Zheng, *ACS Nano*, 2019, **13**, 4560–4571.
139 N. Aratani, D. Kim and A. Osuka, *Acc. Chem. Res.*, 2009, **42**, 1922–1934.

140 C. Wu, X. Guan, J. Xu, Y. Zhang, Q. Liu, Y. Tian, S. Li, X. Qin, H. Yang and Y. Liu, *Biomaterials*, 2019, **205**, 106–119.
141 F. Arcudi, V. Strauss, L. Đorđević, A. Cadranel, D. M. Guldi and M. Prato, *Angew. Chem., Int. Ed.*, 2017, **56**, 12097–12101.
142 M. Managa, O. J. Achadu and T. Nyokong, *Dyes Pigm.*, 2018, **148**, 405–415.
143 H. Zhang, M. A. Bork, K. J. Riedy, D. R. McMillin and J. H. Choi, *J. Phys. Chem. C*, 2014, **118**, 11612–11619.
144 S. Hiroto, Y. Miyake and H. Shinokubo, *Chem. Rev.*, 2017, **117**, 2910–3043.
145 X. Ouyang, X. Wang, H. Kraatz, S. Ahmad, J. Gao, Y. Lv, X. Sun and Y. Huang, *Biomater. Sci.*, 2020, **8**, 1160–1170.
146 D. M. Lopes, J. C. Araujo-Chaves, L. R. Menezes and I. L. Nantes-Cardoso, in *Solid State Physics*, IntechOpen, 2019, pp. 1–20.
147 M. R. Younis, G. He, J. Lin and P. Huang, *Front. Chem.*, 2020, **8**, 1–25.
148 P. Cui and Y. Xue, *J. Mater. Sci.: Mater. Electron.*, 2022, **33**, 5024–5036.
149 M. O. Senge and M. Davis, *J. Porphyrins Phthalocyanines*, 2010, **14**, 557–567.
150 B. Academy, A. N. A. T. P. C. Gomes, M. G. P. M. S. Neves, C. Qu and P. Naturais, *An. Acad. Bras. Cienc.*, 2018, **90**, 993–1026.
151 J. Tian, B. Huang, M. H. Nawaz and W. Zhang, *Coord. Chem. Rev.*, 2020, **420**, 213410.
152 D. Larowska, J. M. O'Brien, M. O. Senge, G. Burdzinski, B. Marciniak and A. Lewandowska-Andralojc, *J. Phys. Chem. C*, 2020, **124**, 15769–15780.
153 D. Qu, M. Zhang, P. Du, Y. Zhou, L. Zhang, D. Li, H. Tan, Z. Zhao, Z. Xie and Z. Sun, *Nanoscale*, 2015, **5**, 12272–12277.
154 F. D'Souza and O. Ito, *Chem. Commun.*, 2009, 4913–4928.
155 O. Penon, M. J. Marín, D. A. Russell and L. Pérez-García, *J. Colloid Interface Sci.*, 2017, **496**, 100–110.
156 E. Chang, J. Bu, L. Ding, J. W. H. Lou, M. S. Valic, M. H. Y. Cheng, V. Rosilio, J. Chen and G. Zheng, *J. Nanobiotechnol.*, 2021, **19**, 1–15.
157 B. K. Walther, C. Z. Dinu, D. M. Guldi, V. G. Sergeyev, S. E. Creager, J. P. Cooke and A. Guiseppi-Elie, *Mater. Today*, 2020, **39**, 23–46.
158 J. Tang, L. Niu, J. Liu, Y. Wang, Z. Huang, S. Xie, L. Huang, Q. Xu, Y. Wang and L. A. Belfiore, *Mater. Sci. Eng. C*, 2014, **34**, 186–192.
159 M. Mahyari, Y. Bide and J. N. Gavgani, *Appl. Catal., A*, 2016, **517**, 100–109.
160 L. Mei, X. Gao, Y. Shi, C. Cheng, Z. Shi, M. Jiao, F. Cao, Z. Xu, X. Li and J. Zhang, *ACS Appl. Mater. Interfaces*, 2020, **12**, 40153–40162.
161 A. Ryan, A. Gehrold, R. Perusitti, M. Pintea, M. Fazekas, O. B. Locos, F. Blaikie and M. O. Senge, *Eur. J. Org. Chem.*, 2011, 5817–5844.
162 R. Chitta and F. D'Souza, *J. Mater. Chem.*, 2008, **18**, 1440–1471.
163 Y. He, M. Garnica, F. Bischoff, J. Ducke, M. L. Bocquet, M. Batzill, W. Auwärter and J. v. Barth, *Nat. Chem.*, 2017, **9**, 33–38.
164 J. Otsuki, *J. Mater. Chem. A*, 2018, **6**, 6710–6753.
165 Y. Xu, Z. Liu, X. Zhang, Y. Wang, J. Tian, Y. Huang, Y. Ma, X. Zhang and Y. Chen, *Adv. Mater.*, 2009, **21**, 1275–1279.
166 D. E. J. G. J. Dolmans, D. Fukumura and R. K. Jain, *Nat. Rev. Cancer*, 2003, **3**, 380–387.
167 J. Baek, T. Umeyama, S. Mizuno, N. v. Tkachenko and H. Imahori, *J. Phys. Chem. C*, 2018, **122**, 13285–13293.
168 N. Nwahara, R. Nkhahle, B. P. Ngoy and J. Mack, *New J. Chem.*, 2018, **42**, 6051–6061.
169 F. Sedona, M. di Marino, M. Sambi, T. Carofiglio, E. Lubian, M. Casarin and E. Tondello, *ACS Nano*, 2010, **4**, 5147–5154.
170 L. C. Nene, M. Managa and T. Nyokong, *Dyes Pigm.*, 2019, **165**, 488–498.
171 S. Moxon, M. Cooke, S. Cox, M. Snow, L. Jeys, S. Jones, A. Smith and L. Grover, *Adv. Mater.*, 2008, **20**, 1727–1731.
172 M. Jokazi, L. S. Mpeta and T. Nyokong, *J. Electroanal. Chem.*, 2021, **901**, 115748.
173 S. Campuzano, P. Yáñez-Sedeño and J. M. Pingarrón, *Nanomaterials*, 2019, **9**, 1–18.
174 C. H. Hendon, A. J. Rieth, M. D. Korzyński and M. Dincă, *ACS Cent. Sci.*, 2017, **3**, 554–563.
175 R. Schneider, M. H. M. Facure, P. A. M. Chagas, R. S. Andre, D. M. dos Santos and D. S. Correa, *Adv. Mater. Interfaces*, 2021, **8**, 2100430.
176 K. Lewandowska, N. Rosiak, A. Bogucki, J. Cielecka-Piontek, M. Mizera, W. Bednarski, M. Suchecki and K. Szaciłowski, *Molecules*, 2019, 24, 688.
177 A. Siklitskaya, E. Gacka, D. Larowska, M. Mazurkiewicz-Pawlicka, A. Malolepszy, L. Stobiński, B. Marciniak, A. Lewandowska-Andrałojć and A. Kubas, *Sci. Rep.*, 2021, **11**, 1–14.
178 R. M. Meudtner, M. Ostermeier, R. Goddard, C. Limberg and S. Hecht, *Chem. – Eur. J.*, 2007, **13**, 9834–9840.
179 K. Ladomenou, V. Nikolaou, G. Charalambidis and A. G. Coutsolelos, *Coord. Chem. Rev.*, 2016, **306**, 1–42.
180 O. J. Achadu, I. Uddin and T. Nyokong, *J. Photochem. Photobiol., A*, 2016, **317**, 12–25.
181 L. C. Nene, M. E. Managa, D. O. Oluwole, D. M. Mafukidze, A. Sindelo and T. Nyokong, *Inorg. Chim. Acta*, 2019, **488**, 304–311.
182 A. Satake, Y. Miyajima and Y. Kobuke, *Chem. Mater.*, 2005, **17**, 716–724.
183 S. Su, J. Wang, J. Qiu, R. Martinez-Zaguilan, S. R. Sennoune and S. Wang, *Mater. Sci. Eng. C*, 2020, **107**, 110313.
184 A. Pallikkara, D. Sebastian and K. Ramakrishnan, *ChemistrySelect*, 2021, **6**, 12224–12232.
185 A. Wojcik and P. v. Kamat, *ACS Nano*, 2010, **4**, 6697–6706.
186 R. A. Sperling and W. J. Parak, *Philos. Trans. R. Soc., A*, 2010, **368**, 1333–1383.

187 T. A. Tabish, C. J. Scotton, D. C. J. Ferguson, L. Lin, A. Van Der Veen, S. Lowry, M. Ali, F. Jabeen, P. G. Winyard and S. Zhang, *Nanomedicine*, 2018, **13**, 1923–1937.
188 D. Iannazzo, C. Celesti and C. Espro, *Biotechnol. J.*, 2021, **16**, 1900422.
189 J. Zeng, K. Q. Chen and Y. X. Tong, *Carbon*, 2018, **127**, 611–617.
190 Y. Yao, E. Ashalley, X. Niu, L. Dai, P. Yu, W. Chen, Z. Qin, L. Zhang and Z. Wang, *Appl. Phys. Lett.*, 2019, **114**, 073101.
191 C. Hu, J. Qu, Y. Xiao, S. Zhao, H. Chen and L. Dai, *ACS Cent. Sci.*, 2019, **5**, 389–408.
192 N. B. Magaela, R. Matshitse, B. Babu, M. Managa, E. Prinsloo and T. Nyokong, *Polyhedron*, 2022, **213**, 115624.
193 P. Chundu, E. Dube, N. Zinyama, M. Moyo, M. Shumba, *et al.*, *Front. Chem.*, 2021, **9**, 633547.
194 Y. Li, T. Y. Lin, Y. Luo, Q. Liu, W. Xiao, W. Guo, D. Lac, H. Zhang, C. Feng, S. Wachsmann-Hogiu, J. H. Walton, S. R. Cherry, D. J. Rowland, D. Kukis, C. Pan and K. S. Lam, *Nat. Commun.*, 2014, **5**, 1–15.
195 O. J. Achadu, M. Managa and T. Nyokong, *J. Photochem. Photobiol., A*, 2017, **333**, 174–185.
196 M. Managa, B. P. Ngoy and T. Nyokong, *New J. Chem.*, 2019, **43**, 4518–4524.
197 R. Matshitse, B. Ngoy, M. Managa, J. Mack and T. Nyokong, *Photodiagn. Photodyn. Ther.*, 2019, **26**, 101–110.
198 T. Bathon, P. Sessi, K. A. Kokh, O. E. Tereshchenko and M. Bode, *Nano Lett.*, 2015, **15**, 2442–2447.
199 D. Wang, L. Niu, Z. Y. Qiao, D. B. Cheng, J. Wang, Y. Zhong, F. Bai, H. Wang and H. Fan, *ACS Nano*, 2018, **12**, 3796–3803.
200 S. Li, S. Zhou, Y. Li, X. Li, J. Zhu, L. Fan and S. Yang, *ACS Appl. Mater. Interfaces*, 2017, **9**, 22332–22341.
201 W. Zhang, A. U. Shaikh, E. Y. Tsui and T. M. Swager, *Chem. Mater.*, 2009, **21**, 3234–3241.
202 A. Chandra, S. Deshpande, D. B. Shinde, V. K. Pillai and N. Singh, *ACS Macro Lett.*, 2014, **3**, 1064–1068.
203 O. J. Achadu and T. Nyokong, *New J. Chem.*, 2017, **41**, 1447–1458.
204 A. Srivatsan, J. R. Missert, S. K. Upadhyay and R. K. Pandey, *J. Porphyr. Phthalocyanines*, 2015, **19**, 109–134.
205 L. Yan, Y. N. Chang, W. Yin, G. Tian, L. Zhou, X. Liu, G. Xing, L. Zhao, Z. Gu and Y. Zhao, *Biomater. Sci.*, 2014, **2**, 1412–1418.
206 N. Nwahara, J. Britton and T. Nyokong, *J. Coord. Chem.*, 2017, **70**, 1601–1616.
207 N. Nwahara, O. J. Achadu, T. Nyokong, R. Nkhahle, B. P. Ngoy, J. Mack, S. Li, S. Zhou, Y. Li, X. Li, J. Zhu, L. Fan, S. Yang, T. Gualberto, B. De Souza, M. Gonçalves, J. Ge, M. Lan, B. Zhou, W. Liu, L. Guo, H. Wang, Q. Jia, G. Niu, X. Huang, H. Zhou, X. Meng, P. Wang, C. Lee, Y. Xuan, R. Zhang, X. X. Zhang, J. An, K. Cheng, Y. Cao, H. Dong, Z. Yang, X. Zhong, Y. Chen, W. Dai, X. X. Zhang, M. Managa, B. P. Ngoy and T. Nyokong, *J. Photochem. Photobiol., A*, 2016, **43**, 6051–6061.
208 C. Y. Lee, O. K. Farha, B. J. Hong, A. A. Sarjeant, S. T. Nguyen and J. T. Hupp, *J. Am. Chem. Soc.*, 2011, **133**, 15858–15861.
209 D. M. Mafukidze and T. Nyokong, *J. Mol. Struct.*, 2019, **1180**, 307–317.
210 L. C. Nene and T. Nyokong, *Photodiagn. Photodyn. Ther.*, 2021, **36**, 102573.
211 P. Zhang and N. Wu, *Chem. Asian J.*, 2017, **12**, 2343–2353.
212 L. Zhang, D. Peng, R. P. Liang and J. D. Qiu, *Anal. Chem.*, 2015, **87**, 10894–10901.
213 D. Peng, L. Zhang, R. Liang and J. Qiu, *ACS Sens.*, 2018, **3**, 1040–1047.
214 O. J. Achadu and T. Nyokong, *Talanta*, 2017, **166**, 15–26.
215 O. J. Achadu and T. Nyokong, *Dyes Pigm.*, 2017, **145**, 189–201.
216 W. Jiang, X. Chen, T. Wang, B. Li, M. Zeng, J. Yang, N. Hu, Y. Su, Z. Zhou and Z. Yang, *RSC Adv.*, 2021, **11**, 5618–5628.
217 W. Jiang, M. Jiang, T. Wang, X. Chen, M. Zeng, J. Yang, Z. Zhou, N. Hu, Y. Su and Z. Yang, *RSC Adv.*, 2021, **11**, 14805–14813.
218 S. Centane, O. J. Achadu and T. Nyokong, *Electroanalysis*, 2017, **29**, 2470–2482.
219 A. R. Monteiro, C. I. V. Ramos, S. Fateixa, N. M. M. Moura, M. G. P. M. S. Neves and T. Trindade, *ACS Omega*, 2018, **3**, 11184–11191.
220 Z. Kamal, M. Z. Ghobadi, S. M. Mohseni and H. Ghourchian, *Biosens. Bioelectron.*, 2021, **188**, 113334.
221 Y. Wang, Z. Hsine, H. Sauriat-Dorizon, R. Mlika and H. Korri-Youssoufi, *Electrochim. Acta*, 2020, **357**, 136852.
222 H. S. Han, H. K. Lee, J. M. You, H. Jeong and S. Jeon, *Sens. Actuators, B*, 2014, **190**, 886–895.
223 O. Adeniyi, N. Nwahara, D. Mwanza, T. Nyokong and P. Mashazi, *Sens. Actuators, B*, 2021, **348**, 130723.
224 H. Dong, W. Gao, F. Yan, H. Ji and H. Ju, *Anal. Chem.*, 2010, **82**, 5511–5517.
225 O. J. Achadu and T. Nyokong, *Dyes Pigm.*, 2019, **160**, 328–335.
226 D. Peng, L. Zhang, R.-P. Liang, J. Qiu, V. A. Online, O. J. Achadu, T. Nyokong, L. Zhang, D. Peng, R.-P. Liang, J. Qiu, O. J. Achadu, T. Nyokong, G. Xue, S. Yu, Z. Qiang, L. Xiuying, L. Jiangrong, O. J. Achadu, T. Nyokong, L. Zhang, D. Peng, R.-P. Liang and J. Qiu, *Dyes Pigm.*, 2017, **166**, 15–26.
227 L. Zhang, D. Peng, R. P. Liang and J. D. Qiu, *Chemistry*, 2015, **21**, 9343–9348.
228 S. R. Nxele and T. Nyokong, *J. Inorg. Biochem.*, 2021, **221**, 111462.
229 Y. Liu, S. Li, K. Li, Y. Zheng, M. Zhang, C. Cai, C. Yu, Y. Zhou and D. Yan, *Chem. Commun.*, 2016, **52**, 9394–9397.
230 P. Sehgal and A. K. Narula, *Opt. Mater.*, 2018, **79**, 435–445.
231 K. H. Koh, S. H. Noh, T. H. Kim, W. J. Lee, S. C. Yi and T. H. Han, *RSC Adv.*, 2017, **7**, 26113–26119.
232 Q. Lu, Y. Zhang and S. Liu, *J. Mater. Chem. A*, 2015, **3**, 8552–8558.

233 Y. Liu, S. Li, K. Li, Y. Zheng, M. Zhang, C. Cai, C. Yu, Y. Zhou and D. Yan, *Chem. Commun.*, 2016, **52**, 9394–9397.
234 Y. Q. Zhang, D. K. Ma, Y. G. Zhang, W. Chen and S. M. Huang, *Nano Energy*, 2013, **2**, 545–552.
235 I. Althagafi and N. El-Metwaly, *Arabian J. Chem.*, 2021, **14**, 103080.
236 M. Ekrami, G. Magna, Z. Emam-Djomeh, M. S. Yarmand, R. Paolesse and C. Di Natale, *Sensors*, 2018, **18**, 1–12.
237 L. Chen, C. Guo, Q. Zhang, Y. Lei, J. Xie, S. Ee, G. Guai, Q. Song, C. Li, *et al.*, *ACS Appl. Mater. Interfaces*, 2013, **5**, 2047–2052.
238 L. L. Li and E. W. G. Diau, *Chem. Soc. Rev.*, 2013, **42**, 291–304.
239 T. Kuila, S. Bose, A. K. Mishra, P. Khanra, N. H. Kim and J. H. Lee, *Prog. Mater. Sci.*, 2012, **57**, 1061–1105.
240 J. Li, T. Li, Y. Duan and H. Li, *Mater. Des.*, 2020, **189**, 108487.
241 P. Arpacay, P. Maity, A. El-Zohry, A. Meindl, S. Akca, S. Plunkett, M. O. Senge, W. J. Blau and O. F. Mohammed, *J. Phys. Chem. C*, 2019, **123**, 14283–14291.
242 F. Paquin, J. Rivnay, A. Salleo, N. Stingelin and C. Silva, *J. Mater. Chem. C*, 2015, **3**, 10715–10722.
243 T. Majumder, S. Dhar, P. Chakraborty, K. Debnath and S. P. Mondal, *J. Electroanal. Chem.*, 2018, **813**, 92–101.
244 M. Dutta, S. Sarkar, T. Ghosh and D. Basak, *J. Phys. Chem. C*, 2012, **116**, 20127–20131.
245 T. Majumder, S. Dhar, P. Chakraborty, K. Debnath and S. P. Mondal, *Nano*, 2019, **14**, 1950012.
246 M. Mojiri-Foroushani, H. Dehghani and N. Salehi-Vanani, *Electrochim. Acta*, 2013, **92**, 315–322.
247 F. Jahantigh, S. M. B. Ghorashi and S. Mozaffari, *J. Solid State Electrochem.*, 2020, **24**, 883–889.
248 S. Kundu, P. Sarojinijeeva, R. Karthick, G. Anantharaj, G. Saritha, R. Bera, S. Anandan, A. Patra, P. Ragupathy, M. Selvaraj, D. Jeyakumar and K. V. Pillai, *Electrochim. Acta*, 2017, **242**, 337–343.
249 P. M. Vijaya, M. P. Kumar, C. Takahashi, S. Kundu, T. N. Narayanan and D. K. Pattanayak, *New J. Chem.*, 2019, **43**, 14313–14319.
250 Y. Li, Y. Zhao, H. Cheng, Y. Hu, G. Shi, L. Dai and L. Qu, *J. Am. Chem. Soc.*, 2012, **134**, 15–18.
251 Q. Li, S. Zhang, L. Dai and L. S. Li, *J. Am. Chem. Soc.*, 2012, **134**, 18932–18935.
252 S. Centane, E. K. Sekhosana, R. Matshitse and T. Nyokong, *J. Electroanal. Chem.*, 2018, **820**, 146–160.
253 N. N. T. Pham, J. S. Park, H.-T. Kim, H.-J. Kim, Y.-A. Son, S. G. Kang and S. G. Lee, *New J. Chem.*, 2019, **43**, 348–355.
254 A. Morozan, S. Campidelli, A. Filoramo, B. Jousselme and S. Palacin, *Carbon*, 2011, **49**, 4839–4847.
255 N. N. T. Pham, S. G. Kang, Y. A. Son, S. Y. Lee, H. J. Kim and S. G. Lee, *J. Phys. Chem. C*, 2019, **123**, 27483–27491.
256 Y. Liu and P. Wu, *ACS Appl. Mater. Interfaces*, 2013, **5**, 3362–3369.
257 M. Jahan, Q. Bao and K. P. Loh, *J. Am. Chem. Soc.*, 2012, **134**, 6707–6713.
258 S. Kumar, R. K. Yadav, K. Ram, A. Aguiar, J. Koh and A. J. F. N. Sobral, *J. CO2 Util.*, 2018, **27**, 107–114.
259 S. Su, J. Wang, E. Vargas, J. Wei, R. Martínez-Zaguilán, S. R. Sennoune, M. L. Pantoya, S. Wang, J. Chaudhuri and J. Qiu, *ACS Biomater. Sci. Eng.*, 2016, **2**, 1357–1366.
260 M. Mahyari, Y. Bide and J. N. Gavgani, *Appl. Catal., A*, 2016, **517**, 100–109.
261 M. Mahyari and J. Nasrollah Gavgani, *Res. Chem. Intermed.*, 2018, **44**, 3641–3657.
262 X. Weng, H. Ye, W. Xie, M. Ying, H. Pan and M. Du, *Nanoscale Adv.*, 2021, **3**, 3900–3908.
263 D. Kim, J. Byun, J. Park, Y. Lee, G. Shim and Y. K. Oh, *Biomater. Sci.*, 2020, **8**, 1106–1116.
264 Y. Luo, J. Liu, Y. Liu and Y. Lyu, *J. Polym. Sci., Part A: Polym. Chem.*, 2017, **55**, 2594–2600.
265 A. C. Lannes, B. Leal, J. S. Novais, V. Lione, G. C. T. S. Monteiro, A. L. Lourenço, P. C. Sathler, A. K. Jordão, C. R. Rodrigues, L. M. Cabral, A. C. Cunha, V. Campos, V. F. Ferreira, M. C. B. V. De Souza, D. O. Santos and H. C. Castro, *Curr. Microbiol.*, 2014, **69**, 357–364.
266 I. Paramio, T. Torres and G. de la Torre, *ChemMedChem*, 2021, **16**, 2441–2451.
267 S. Su, J. Wang, J. Wei, R. Martínez-Zaguilán, J. Q. and S. W. , *New J. Chem.*, 2015, **39**, 5743–5749.
268 B. Kulyk, K. Waszkowska, A. Busseau, C. Villegas, P. Hudhomme, S. Dabos-Seignone, A. Zawadzka, S. Legoupy and B. Sahraoui, *Appl. Surf. Sci*, 2020, **533**, 147468.
269 D. Suhag, A. K. Sharma, P. Patni, S. K. Garg, S. K. Rajput, S. Chakrabarti and M. Mukherjee, *J. Mater. Chem. B*, 2016, **4**, 4780–4789.
270 S. Wang, I. S. Cole and Q. Li, *RSC Adv.*, 2016, **6**, 89867–89878.
271 M. Chen and Q. Chen, *Biomater. Sci.*, 2020, **8**, 5846–5858.
272 T. A. Tabish, S. Zhang and P. G. Winyard, *Redox Biol.*, 2018, **15**, 34–40.
273 H. Y. Fan, X. H. Yu, K. Wang, Y. J. Yin, Y. J. Tang, Y. L. Tang and X. H. Liang, *Eur. J. Med. Chem.*, 2019, **182**, 111620.
274 F. D'Souza, S. K. Das, M. E. Zandler, A. S. D. Sandanayaka and O. Ito, *J. Am. Chem. Soc.*, 2011, **133**, 19922–19930.
275 N. Zhang, L. Wang, H. Wang, R. Cao, J. Wang, F. Bai and H. Fan, *Nano Lett.*, 2018, **18**, 560–566.
276 Y. Cao, H. Dong, Z. Yang, X. Zhong, Y. Chen, W. Dai and X. Zhang, *ACS Appl. Mater. Interfaces*, 2017, **9**, 159–166.
277 A. T. P. C. Gomes, R. Fernandes, C. F. Ribeiro, J. P. C. Tomé, M. G. P. M. S. Neves, F. de C. da Silva, V. F. Ferreira and J. A. S. Cavaleiro, *Molecules*, 2020, **25**, 1607.
278 C. Wang and Y. Qian, *Biomater. Sci.*, 2020, **8**, 830–836.
279 Y. Zhang, N. Qiu, Y. Zhang, H. Yan, J. Ji, Y. Xi, X. Yang, X. Zhao and G. Zhai, *Biomater. Sci.*, 2021, **9**, 3989–4004.
280 B. Yang, K. Wang, D. Zhang, B. Sun, B. Ji, L. Wei, Z. Li, M. Wang, X. Zhang, H. Zhang, Q. Kan, C. Luo, Y. Wang, Z. He and J. Sun, *Biomater. Sci.*, 2018, **6**, 2965–2975.
281 X. Li, *Physiol. Behav.*, 2016, **176**, 139–148.

282 M. D'Ambrosio, A. C. Santos, A. Alejo-Armijo, A. J. Parola and P. M. Costa, *Mar. Drugs*, 2020, **18**, 1–14.
283 Z. G. Wang, R. Zhou, D. Jiang, J. E. Song, Q. Xu, J. Si, Y. P. Chen, X. Zhou, L. Gan, J. Z. Li, H. Zhang and B. Liu, *Biomed. Environ. Sci.*, 2015, **28**, 341–351.
284 H. M. Wang, J. Q. Jiang, J. H. Xiao, R. L. Gao, F. Y. Lin and X. Y. Liu, *Chem.-Biol. Interact.*, 2008, **172**, 154–158.
285 W. Park, S. Cho, J. Han, H. Shin, K. Na, B. Lee and D.-H. Kim, *Biomater. Sci.*, 2018, **6**, 79–90.
286 M. Saeed, W. Ren and A. Wu, *Biomater. Sci.*, 2018, **6**, 708–725.
287 P. Sen and T. Nyokong, *Photodiagn. Photodyn. Ther.*, 2021, **14**, 102300.
288 Y. I. Openda, P. Sen, M. Managa and T. Nyokong, *Photodiagn. Photodyn. Ther.*, 2020, **29**, 101607.
289 A. E. O'Connor, W. M. Gallagher and A. T. Byrne, *Photochem. Photobiol.*, 2009, **85**, 1053–1074.
290 N. Nwahara, R. Nkhahle, B. P. Ngoy, J. Mack and T. Nyokong, *New J. Chem.*, 2018, **42**, 6051–6061.
291 D. M. Lopes, J. C. Araujo-Chaves, L. R. Menezes and I. L. Nantes-Cardoso, *Solid State Physics Metastable, Spintronics Materials and Mechanics of Deformable Bodies: Recent Progress*, IntechOpen, UK, 2019, DOI: 10.5772/intechopen.78485.
292 M. Steenhuis, F. Corona, C. M. T. Hagen-Jongman, W. Vollmer, D. Lambin, P. Selhorst, H. Klaassen, M. Versele, P. Chaltin and J. Luirink, *ACS Infect. Dis.*, 2017, **8**, 2250–2263.
293 S. Kirar, N. S. Thakur, J. K. Laha and U. C. Banerjee, *ACS Appl. Bio Mater.*, 2019, **2**, 4202–4212.
294 J. Feng, Y. L. Yu and J. H. Wang, *New J. Chem.*, 2020, **44**, 18225–18232.
295 J. Oyim, C. A. Omolo and E. K. Amuhaya, *Front. Chem.*, 2021, **9**, 1–15.
296 J. Chen, Y. Cui, K. Song, T. Liu, L. Zhou, B. Bao, R. Wang and L. Wang, *Biomater. Sci.*, 2021, **9**, 2115–2123.
297 Y. Zhang, J. Ma, D. Wang, C. Xu, S. Sheng, J. Cheng, C. Bao, Y. Li and H. Tian, *Biomater. Sci.*, 2020, **8**, 6526–6532.
298 M. Qindeel, S. Sargazi, S. M. Hosseinikhah, A. Rahdar, M. Barani, V. K. Thakur, S. Pandey and R. Mirsafaei, *ChemistrySelect*, 2021, **6**, 14082–14099.
299 N. Nwahara, O. J. Achadu and T. Nyokong, *J. Photochem. Photobiol., A*, 2018, **359**, 131–144.
300 Z. Liu, T. Cao, Y. Xue, M. Li, M. Wu, J. W. Engle, Q. He, W. Cai, M. Lan and W. Zhang, *Angew. Chem., Int. Ed.*, 2020, **59**, 3711–3717.
301 S. Li, Q. Zou, Y. Li, C. Yuan, R. Xing and X. Yan, *J. Am. Chem. Soc.*, 2018, **140**, 10794–10802.
302 E. Zenkevich, T. Blaudeck, V. Sheinin, O. Kulikova, O. Selyshchev, V. Dzhagan, O. Koifman, C. V. Borczyskowski and D. R. T. Zahn, *J. Mol. Struct.*, 2021, **1244**, 131239.
303 S. R. Nxele and T. Nyokong, *Dyes Pigm.*, 2021, **192**, 109407.
304 D. M. Mafukizde and T. Nyokong, *J. Coord. Chem.*, 2017, **70**, 3598–3618.
305 F. Wu, L. Yue, H. Su, K. Wang, L. Yang and X. Zhu, *Nano Express*, 2018, **13**, 1–10.